Title: From population trends to biodiversity changes: synthesizing multi-species signals of collapse

Author names: Katherine Hébert[1,2], Alexandre Fuster-Calvo[2], Camille Lévesque[2], Dominique Gravel [2].

Author affiliations:

[1] Department of Biology, McGill University, Québec, Canada.

[2] Département de biologie, Université de Sherbrooke, Sherbrooke, Canada.

Corresponding author: Katherine Hébert (katherine.hebert@mail.mcgill.ca)

Keywords: biodiversity change, biodiversity indicator, species abundance, covariance, community stability, joint modeling, Atlantic cod.

Word count: 3726

Acknowledgements

K.H. was supported by Natural Sciences and Engineering Research Council of Canada (NSERC) and the Fonds de recherche du Québec Nature et Technologie (FQRNT). We thank Laura J. Pollock, Eric Pedersen, Fanie Pelletier, and Théo Garnier for insightful discussions and feedback on earlier versions of the manuscript.

Abstract

Taking the pulse of biodiversity is no small feat, and abundance time series are some of the most valuable data we have to measure change. Biodiversity changes are often complex, with some species declining while others grow, leading to a reorganisation of the network of interactions between species. The infamous decline of Atlantic cod in the Newfoundland shelf groundfish community between 1981 and 2013 is an example of such complexity. Here, we develop a new approach to track the multispecies signals before and after the cod decline, offering a community-oriented alternative to species abundance indicators like the Living Planet Index. We derive theory-based indicators and build a model to quantify the short-term stability and long-term reorganisation of communities with an explicit estimation of uncertainty. These indicators together reveal how severe declines in dominant species like Atlantic cod, combined with community-wide biomass changes, generated periods of instability and recovery that reshuffled the community more profoundly than previously thought. We find that the community was already facing reorganisation before the collapse and only recently recovered towards a desired state. By grounding indicators in ecological theory, we are better equipped to understand the process, and not just the pattern, of change.

Introduction

Biodiversity change is unfolding as a balance between "winners" and "losers" [1,2], where species are growing or declining as they navigate changes in their environment and their community[3]. These changes reshuffle species' abundances within communities, which alter species interactions, ecosystem functioning, and lower resilience[4–6] . Despite mounting calls to move past species-centric metrics for conservation[7,8], biodiversity change assessments still typically flatten the variability between species into an average, ignoring the collective implications[9,10] of species-level changes for community stability.

To link species-level changes to community stability, we must adopt multispecies metrics of biodiversity change. For example, the Living Planet Index (LPI), which is part of the Global Biodiversity Framework's monitoring program to track progress towards global biodiversity targets[11], synthesizes over 30,000 vertebrate population trends into an average global trend of relative species abundances since 1970[11,12]. Indicators like the LPI rely on the assumption that populations (and species) vary independently and therefore estimate species' trends separately before averaging them. However, species' abundances are often correlated because of their ecological relatedness[13–15] and their proximity in time and space[16,17], and ignoring these correlations distorts average trends[18,19].

Considering these correlations is not only a statistical problem: without them, we cannot understand how species' trends scale up to impact community stability. At the species level, abundance trends reflect vulnerability to extinction, where declines and rising variance are both signals of increasing extinction risk[20–22]. These species-level changes then scale up to drive community dynamics through the correlated variance (or, covariance) between species' trends at both short (e.g., annual) and longer (e.g., decade or longer) time scales. In the short-term,

positive correlations between species' interannual fluctuations can amplify their impact at the community level, potentially generating unstable dynamics[23,24], while negative covariances can generate compensatory dynamics which can stabilize communities[25,26]. Correlations between species' long-term trends then indicate how coordinated directional changes across species-arising from shared environmental responses, interactions, or common pressures[4,27] combine to reshuffle community structure. At any time scale, correlations between species ultimately manifest as community-level variance, which reflects the overall breadth of gains and losses unfolding throughout the community – where strong correlations and high variance typically indicate drastic community-level change[28]. At short time scales, these correlations determine how fluctuations propagate through the community (i.e., whether they are buffered or amplified). Increases in variance indicate that fluctuations are not effectively buffered across species, so that their effects accumulate at the community level, amplifying variability and signaling unstable dynamics. Over longer time scales, correlations instead shape how these dynamics accumulate into lasting reorganization of community structure. Accordingly, long-term variance reflects sustained differences in species' trajectories, indicating reshuffling of species abundances that can profoundly alter community functioning[29] (Fig. 2). In a practical sense, variance also indicates that species deviate widely from the community-level average trend, and therefore that an average is not a representative summary of these changes.

Joint models make it possible to track these multispecies signals of biodiversity change by explicitly linking species trends to community-level changes. By pushing past the long-standing statistical assumption that species vary independently, joint models have already led to breakthroughs in modeling and monitoring biodiversity[30–32], including species distribution modelling[33,34], community ecology[35], and species trend assessments[36] and forecasting[37,38]. Latent

variables are key to these advances – they represent unmeasured predictors that leave imprints on observed dynamics, such as species interactions[39] or correlated responses to environmental conditions[40]. Latent variables capture residual correlations between trends[30,40], which reflect associations between species and how they are changing[41] – making it possible to simultaneously estimate species-level and community-level trends and species associations in one model.

We propose a framework to collectively summarise species-level to community-level changes from abundance time series (Fig. 1). We develop a general joint model to estimate changes in abundance over time for a community of species, composed of three elements: (1) a multispecies temporal trend of abundance through time, (2) a latent trend, and (3) a residual error term (Fig. 1). First, species' temporal trends are estimated jointly from a community-level distribution, defined by an average community-level rate of change and variance in abundance. This community distribution can be assessed per time step to build a timeline of community stability. Second, the latent trend captures residual correlations between species that reflect associations between species' trends[40]. The model's residual error then captures the remaining unexplained variation from processes like measurement uncertainty and demographic and environmental stochasticity that drive species' dynamics[42–45].

From this model, we derive three indicators of biodiversity change: (1) the Community Change Index (CCI), summarising overall average change in community-level abundance and community, (2) a multi-species trajectory of instantaneous rates of change (Community Abundance Index, CAI), and (3) the variance across species' trajectories (Community Stability Index, CSI), which we interpret alongside species associations at short and long-term scales. Together, these indicators summarize the ecological implications of species-level abundance changes on community stability. In an undisturbed system, the Community Change, Community

Abundance, and Community Stability indices should all remain low[46]. Departures from zero in the Community Change and Community Abundance indices reveal absolute change in community-level abundance, while sustained increases in the Community Stability Index (and in the strength of pairwise species' correlations) essentially signal community instability at short-term scales and reshuffling at long-term scales (and potentially, regime shifts)[46]. We demonstrate this approach on the Newfoundland shelf groundfish community between 1981 and 2013, in which the extreme decline in several species (most notably the Atlantic cod, i.e., *Gadus morhua*) deeply restructured the community[47]. We compare the Community Abundance Index with the Living Planet Index to highlight the conceptual and statistical benefits of a multispecies approach to understand and track abundance changes.

Learning from the past: the Newfoundland shelf groundfish community

In the late 1980s to early 1990s, the overexploitation of Atlantic cod (*Gadus morhua*) contributed to a major trophic cascade in the northwest Atlantic ecosystem[48]. *Gadus morhua* declined severely to biomass levels that were 99.9% smaller than in 1983 as of 2001[49]. Because cod consume a wide variety of prey[50] and are themselves predated by other fish, marine mammals, birds, and invertebrates[51], this dramatic decline had rippling effects throughout the entire marine ecosystem. These effects were further amplified by synchronized declines[47] in other commercial fish (halibut, plaice, and redfish)[47,51], resulting in accelerated biomass losses throughout the community. Since the early 2000s, biomass has gradually increased though recovery has been slowed in part due to seal predation pressure[52,53] – and *Gadus morhua* is still classified as "Endangered" in the Newfoundland Shelf[51].

This example of a community before, during, and after its near collapse offers a unique example of complex biodiversity changes[46]: that is, the rapid and severe declines between the mid-1980s and mid-1990s, the slow recovery of some (but not all) species into the 2000s and 2010s, and most importantly – how species-level changes scale up to drive community-level change.

Results

Community Change Index (CCI)

The Community Change Index (CCI) tracks the average (i.e., absolute change) and variance (i.e. degree of reshuffling) of the full distribution of estimated annual rates of change across all species in the Newfoundland shelf groundfish community between 1981 and 2013 (Fig. 3a). This indicator (μ_α = -0.005, SD = 0.10) shows that the average species lost 0.5% of their baseline biomass annually, but its variance component (σ_α^2 = 0.010) is relatively high, which is essential to interpret this indicator: (1) the average is a poor indicator of community-level change, and (2) species underwent large gains and losses, ranging between -33% declines to 29% growths (Fig. 3a), which reshuffled the community between 1981 and 2013 (as in Fig. 2).

Community Abundance Index (CAI)

The Community Abundance Index (CAI) then summarises species-level and community-level changes through time: the most dramatic declines happened during the 1980s, followed by the largest biomass gains in the mid-2000s (Fig. 3b). The CAI followed a consistently negative trend during the 1980s, then alternated between slow growths and slow declines during the 1990s and

2000s (Fig. 3b). Between 1981 and 1988, an average species in the community lost between 2.48% of their biomass annually (in 1982, 90% CI = -26% to 22%) and 5.83% (in 1985, 90% CI = -34.0% to 26.1%), resulting in a total loss of 29.7% of their baseline biomass during this period. The large variability around the average trend captures large losses and large gains in the relative abundance of species within the community, particularly between 1981 and 2000 (Fig. 3b). This uncertainty interval shows the residual variation from stochastic (demographic and environmental fluctuations) and measurement (observation and data recording) processes, which were propagated from data to indicator – but importantly, without the uncertainty (residual correlations between species) captured with the latent model (Fig. S6).

Community Stability Index (CSI)

The variance of this trend – i.e., the community stability index (CSI) – is critical to reveal how species-level changes combine to profoundly reshuffle the community. Community structure underwent profound changes between 1981 and 2013 (Fig. 3c), with the highest variability between 1981 and 1990 (CSI: 0.14 to 0.17), just before the collapse. Though the community regained some stability during the early 2000s, species' trends remained variable during the late 2000s until 2013 (Fig. 3c). This large variability in species' trends indicates the strong reshuffling of the community due to the collapse of commercially fished species in the 1980s and 1990s, which persist during the slow and variable recovery of species' biomasses in the decades that follow. If these species' trends were assessed as an average trend across species without this joint model structure, these changes in community-level variation would be missed, and the community's stability would risk being overestimated.

The rate of change in biomass varied widely across and within species between 1981 and 2013. Species varied widely in their median annual rates of change, and all underwent periods of decline and growth, though to different extents (Fig. S7). Though all species were weighted to inform the model equally, species that represented a large portion of the community's baseline biomass underwent greater losses and gains than less abundant species (Fig. S7b), and their fluctuations have a potentially greater effect on ecosystem stability. Atlantic cod (*Gadus morhua*) which underwent the community's most extreme decline (– 8.4% median decline per year, 90% CI: -20.3% to 11.6%) (Fig. S7a), which is particularly dangerous because cod was the most abundant species in the baseline community, representing over 30% of the community's biomass in 1981 (Fig. S7b). Though cod biomass declined overall, the model also captures the large variability within this species ($\mu_{\alpha i}$ = -7.0%, SD = 0.09), including its slow recovery during the 2000s (Fig. S7a). Many species demonstrated a similarly large variance in their annual rates of change during this period, including declining species like *Raja radiata* ($\mu_{\alpha i}$ = -8.9%, SD = 0.12) and *Anarhichas denticulatus* ($\mu_{\alpha i}$ = -7.8%, SD = 0.12), which also represented large portions of the community's biomass. Though increasing species like *Enchelyopus cimbrius* ($\mu_{\alpha i}$ = 7.7%, SD = 0.12) and *Urophycis chesteri* ($\mu_{\alpha i}$ = 7.2%, SD = 0.15) also varied in their rates of change, they typically represented a much smaller proportion of the community biomass (Fig. S7b), and their gains were therefore not comparable to the losses in more dominant species.

A community's trajectory from near collapse to complex recovery dynamics

Together, these three indicators (CCI, CAI, CSI) summarise the trajectory of the community's dynamics (Fig. 3d) and can interpreted collectively to identify periods of absolute biomass change and community reshuffling (Fig. 2). Overall, the CCI (Fig. 3d; bottom-left quadrant)

indicates that the community exhibited widespread declines and community reshuffling (see Fig. 2, bottom-left quadrant) between 1981 and 2013. The CAI and CSI then reveal a more complex timeline of changing dynamics (Fig. 3d), starting with over a decade of instability marked by severe declines with strong reshuffling from at least 1981 to 1989, followed by sustained though lighter reshuffling until the mid-1990s. From the mid-to-late 1990s and most of the 2000s, the indicators show the complexity of recovery after drastic community change: dynamics remain highly variable though out of the 'danger zone' (i.e., the bottom-left quadrant), bouncing between periods of growth (Fig. 3d; top-right) and decline (Fig. 3d; top-left). A sharp return to growth-with-reshuffling dynamics in the mid-2000s (bottom-right) and absolute growth in the late 2000s (top-right) indicate early though variable signs of recovery. Though the community's biomass continues to grow and sometimes decline from 2007 onwards, the drastic reshuffling in prior years is irreversible: the community is fundamentally altered from its pre-1981 structure and dynamics.

Short-term and long-term species associations

The residual pairwise correlations between species' biomass variations reflect the dynamics that underpin short-term community stability. In the groundfish community, species' short-term dynamics were strongly correlated (both positively and negatively) between 1981 and 2013 (Fig. 4a,c), signaling large, widespread short-term variability in biomass that reflects community instability. Short-term correlations were strongest prior to and during the collapse (Fig. S8), allowing perturbations to propagate across the community and amplify aggregate variability, and weakened during the beginning of the recovery period. Long-term correlations, which are the pairwise product of species' overall trajectories (i.e., their linear slopes; see Fig. S9), indicate

how species' overall trajectories combine to reshuffle the community's structure (Fig. 4b,d) and highlight species whose relative positions shifted most dramatically within the community (Fig. S10). For example, strong positive short-term and long-term correlations between declining and dominant species like *Gadus morhua*, *Raja radiata*, *Hippoglossoides platessoides*, *Anarhichas denticulatus*, and *Sebastes marinus* (Fig. 4a,b), are notably strong signals of a sustained, absolute decline in community biomass and a profound shift in community structure during this period. See Supp. Mat. S1 for more details about leveraging the model's latent variable component to understand species dynamics and responses to potential drivers of change.

Box 1. A multispecies alternative to the Living Planet Index

The Living Planet Index (LPI) summarizes changes in the abundance of separately modeled species relative to a baseline[12], while the Community Abundance Index (CAI) jointly estimates the rate of change in species' abundances through time. When applied to the Newfoundland groundfish community between 1981 and 2013, both the LPI and the CAI capture the biomass collapse in the 1980s and 1990s (Fig. 5a) – with some key distinctions. While the LPI estimates that an average species lost around 80% of its biomass between 1981 and 1994 (LPI: 19.6%, CI: 14.5% to 26.9%), the CAI shows a more moderate average loss of around 50% with wider variation across species, ranging from 25% to 61% relative losses (CAI: 52.3%, CI: 38.3% to 74.4%). Both indicators then show a slow recovery of the community until 2013, where the LPI shows that species recovered to around half of their baseline biomass (LPI: 56.3%, CI: 32.0% to 95.4%) while the CAI shows an average recovery to ~25% of the baseline biomass (CAI: 72.8%, CI: 48.6% to 103.3%) (Fig. 5b).

The indicators' uncertainty intervals tell a very different story: they represent different sources of variability and therefore differ substantially in the degree of confidence they communicate. The LPI's intervals represent the range of species' trends around the average within its sample – but do not reflect how the variability in the raw data (and how it is processed) affects confidence in the average trend[19] (Fig. 5a). The CAI's intervals instead represent full propagated variation from the raw data to the final indicator, indicating a more comprehensive estimation of confidence in the average trend (Fig. 5b). Where the LPI's narrow intervals suggest that all species in the community were declining drastically during the 1980s and 1990s (Fig. 5), the CAI's intervals capture the wider variability in species' trends that shows both the large gains and losses (Fig. S7) – meaning the indicator signals both absolute abundance changes and profound restructuring of the community.

Discussion

Integrating ecological theory into the design and interpretation of biodiversity indicators is key to understanding the process – and not just the pattern – of biodiversity change. We proposed an alternative approach to additive indicators to summarise the collective implications of species' trends for community stability, deriving three complementary indicators of change (Fig. 1): (1) a Community Change Index (CCI), which summarises community-level change in biomass and structure, which can then be broken down into (2) a Community Abundance Indicator (CAI), which summarises average annual species-level changes through time while accounting for species associations, and (3) a Community Stability Index (CSI), which is the variance across species' trends. We then draw insights from the estimated (4) species associations that moderate

community stability and reshuffling. By jointly summarising species trends (Fig. 3d), we can build a more comprehensive and explicitly multi-species portrait of biodiversity change.

When species' trends are aggregated together additively (as in Box 1), species-level changes cannot be linked to higher-level changes in community structure that regulate ecosystem function. For example, though the LPI detects the large declines in dominant species within the community (Fig. 5), its uncertainty intervals generate a false impression that all species were declining. This situation is particularly dangerous if an average trend appears to show no net change because large declines are offset by large gains in some species, as occurred in the Newfoundland shelf groundfish community (Fig. 3). An average trend also flattens the variability that underlies the first signals of recovery in many species during the 2000s and 2010s, which flags that the ecosystem is still far from stable despite the average abundance growth within the community. Average trends must be interpreted alongside their variance to avoid decisions taken under a false sense of ecological stability, and without foresight about the potential repercussions of reshuffled communities.

A joint model-based indicator approach opens the possibility of leveraging species associations to better understand the dynamics underlying an overall trend and their potential implications for ecosystem stability (Fig. 1). The short-term and long-term correlations between species' biomass trends in the Newfoundland shelf groundfish community (Fig. 4) are consistent with the prevalent synchronization of species' responses to the pressure of overfishing, predator-prey relationships, and changes in temperature[47]. Long-term correlations are particularly informative to understand the outcomes of many years of abundance changes relative to the baseline community's structure. In relatively stable communities, species' long-term trajectories should remain weakly correlated and close to zero, indicating limited directional change. In

contrast, strong long-term correlations reveal coordinated, directional shifts in species abundances, signaling a reorganization of community structure that can fundamentally alter community composition and functioning[54] (Fig. S10). From a statistical perspective, this approach has the added benefit of accounting for more residual variation (Fig. S6), which (1) allows for more certain predictions (which improve the precision of derived indicators), and (2) explicitly accounts for correlated residual variation that are critical to reliably summarise trends across multiple non-independent species[18], particularly for abundance indicators like the Living Planet Index[19].

Accurate uncertainty assessments are critical to ensure that indicators are used appropriately for decision-making[55–57], but uncertainty is typically under-represented in indices of abundance changes[18]. This creates an impression that averaged abundance trends are more certain than they are[18,19] (see Box 1). Joint modelling approaches inherently propagate uncertainties from data to estimated trend, which clarifies the level of confidence that can be placed in the average trend (or, indicator) to avoid overconfidence in estimations of change[58].

To be an effective tool, indicators of biodiversity change must also relate to the ecological reality that they are intended to monitor. The Living Planet Index has been repeatedly misinterpreted as a metric of population abundance, though it measures the *relative abundance* of an average population rather than the average change in the *number of individual animals* in a population[59]. This distinction is difficult to communicate because it requires an understanding of relative abundance, which can easily mislead interpretations of the LPI's message[11]. Instead, deriving indicators directly from the estimated absolute rate of change in abundance retains the link between the metrics and the reality (and units) they are intended to represent.

It is increasingly clear that we must move towards a multispecies view to understand, track, and act on biodiversity change[7]. Species abundance is one of the essential building blocks to measure and monitor biodiversity change[60], and is particularly valuable for early change detection to inform early and effective conservation measures[61]. Data constraints will of course restrict the application of our proposed approach at broad scales, though the increasing availability of assemblage time series (e.g., BioTIME[62]) offers promising opportunities to unpack species-to-community signals of change. However, the proposed approach's greatest potential is to unpack changes at finer scales, which are where we can understand, act on, and eventually, attribute[63] changes to their drivers (see Supp. Mat. S1). This multi-species approach bridges two gaps between indicators and their conservation and policy implications: (1) the growing prioritization of an ecosystem approach in global biodiversity policy frameworks (e.g. Global Biodiversity Framework[64]), echoed by recent calls for more mechanistic approaches to conservation[7,8] and, (2) the urgent need for indicators at the finer scales needed to inform their practical use for conservation and management[65]. The approach developed here provides a theoretical and statistical framework to address these needs by uncovering community dynamics that are invisible when species are assessed separately, but essential to capture the implications of changes on ecosystem health.

Conclusion

Biodiversity change is progressing as a reorganization of species within communities that are responding to changing environmental conditions and to each other. Capturing this reorganization is critical to monitor biodiversity change effectively. Abundance-based

summaries of biodiversity change must consider each species as a part of a whole to reflect this reorganization and its ecological implications, and therefore to be informative indicators of biodiversity change. The variability at the species, between-species, and community levels are each pivotal pieces of the puzzle to detect the structural changes in biodiversity which pose a risk to community stability, and here we outline a framework to translate these signals into interpretable indicators of multispecies abundance change. This approach reveals a more complex portrait of a community near collapse and in early recovery than what was previously known: the Atlantic cod's community was already being profoundly reshuffled by 1981, and this reorganization continued for over a decade until reaching a relatively more desirable state. However, the drastic changes in biomass across species had ripple effects throughout the community and its food web, altering energy flows throughout the ecosystem. Though aggregated trends are useful to summarise large quantities of data quickly and simply, they cannot capture such changes in the species and community dynamics that underly biodiversity changes. Theoretical, statistical, and computational developments now allow us to efficiently disentangle these signals of change across ecological scales to better understand, track, and hopefully, prevent biodiversity change. Doing so can help us move towards a more comprehensive portrait of biodiversity change, to reveal the causes and implications of species-level changes on community stability and ultimately, ecosystem functioning to better inform conservation policy and action.

Methods

Defining a general multispecies joint model of abundance change

We modelled species abundances through time (N_t) using a joint model that, in its most general form, is composed of a temporal trend of abundance through time, a latent trend, and residual error (Fig. 1):

$$N_{i,t} = f(t, \alpha_{i,t}) + g(z, \lambda_{i,t}) + \varepsilon_{i,t} \quad \text{(eq. 1)}$$

The first part of this model, $f(t, \alpha_i)$, is a function of time *t* that estimates the temporal trend in the abundance of each species *i* (α_i). Each species' trend can then be thought of as a sample from the community-level distribution of trends:

$$\alpha_{i,t} = N(\mu_{\alpha,t}, \sigma^2_{\alpha,t}) \quad \text{(eq. 2)}$$

Where $\mu_{\alpha,t}$ is the average rate of change in abundance across all species at each time t, which is an index of abundance change, and where $\sigma^2_{\alpha,t}$ is the variance in the rates of change among species at each time *t*, which is an index of community stability. This distribution of estimated rates of change can be assessed for each time step *t* to determine the average trend and variance in abundance across all species at each time step to obtain a timeline of community stability, or over the entire period to summarize this stability.

The second part of this model, $g(z, \lambda_{i,t})$, estimates the variability in abundance that is due to unobserved "latent" predictors (*z*). Each species' relationship with the latent predictors is estimated as factor loadings at each time step ($\lambda_{i,t}$), which capture the correlated fluctuations between species' abundance trends. Without this latent function, the residual covariation between species would be part of the residual error ($\varepsilon_{i,t}$), where it would contribute to the

uncertainty around the trend rather than contributing to the estimation of the abundance trend (Warton et al., 2015).

The third part of the model is its uncertainty, which is the residual error ($\sum_{i,t}$) that contains the species-specific variation in species' abundances which is unexplained by the predictors and the latent factors at each time step. This residual variation includes signals of measurement uncertainty, along with the demographic and environmental stochasticity that generate variability in species' abundances.

Hierarchical dynamic generalized additive model (DGAM)

We demonstrated this general model in the form of a hierarchical Bayesian dynamic generalized additive model (DGAM), which jointly estimates trends in multiple time series with a dynamic latent component that captures residual correlations between species' trends[37]. This model is conceptually analogous to approaches like hierarchical modelling of species communities (HMSC) and joint species distribution models that share information across species to estimate joint responses to unmeasured "latent" predictors[35,40,66] . A critical feature of DGAMs is the dynamic latent component of the model, which evolves over time to capture associations between species that may change throughout the time series[37].

We specified the model in the form of a DGAM as follows for species (*j*) and for time steps (*t*):

$$E(N_{i,t}) = \beta_{0,i} + \sum_{j=1}^{J} \beta_j s_j(t) + \sum_{m=1}^{M} (z_m, \lambda_{i,t}) + \varepsilon_{i,t} \quad \text{(eq. 3)}$$

where $E(N_{i,t})$ is the estimated abundance *N* for species *i* at time *t*, and $\beta_{0,i}$ is a species-specific intercept. The temporal component of the model consists of *j* smoothed basis functions at time *t*, multiplied by species-specific coefficients β_j, which estimates the global temporal trend jointly

for all species. The basis functions were derived with thin plate splines using nine knots, which is one knot every four years. The latent component of the model is a product of z_m, which are estimates for M temporal latent predictors (z_m), and $\lambda_{i,t}$, which are the species' latent factor loadings at each time t. To capture the latent temporal dynamics in species' abundances, we specified the latent trend model as a smooth function in the form of a Gaussian process. The model estimated between $M = 2$ and $M = 15$ (half the total number of time series) latent predictors and increasingly penalized them to squeeze un-needed variables into flat lines, effectively removing them from the model[37]. As a result of this procedure, the model retained $M = 2$ latent predictors (Fig. S4), which accounted for more of the residual variation in the community's biomass through time compared to the same model specified without a latent trend component (Fig. S6).

Data: The Newfoundland shelf groundfish community

We applied this model to estimate the average trend in species' biomasses of the groundfish community off the coast of Newfoundland in the North Atlantic between 1981 and 2013[47]. Abundance was measured as biomass in kilograms per trawl of each species, which were recorded as part of a random depth-stratified survey with fixed duration and speed trawls[47]. The dataset used in this study consists of the average yearly biomass for all trawls of 29 groundfish species in the North Atlantic Fishing Organization (NAFO) divisions 2J, 3K, and 3L[47]. The dataset excludes species that were sensitive to a gear change from 1995 onwards, when the introduction of a smaller mesh size captured more small-bodied fish[47]. To fit the model, we centered all species' biomasses on their baseline biomass in 1981 and divided this difference in

biomass by each species' mean biomass to model the normalized difference in each species' abundance from the start of the time series.

Model fitting

We fit the model with the *mvgam* package (version 1.0.5.) in R, which uses Hamiltonian Monte Carlo to estimate all parameters in Stan. We ran the model for 15000 iterations with the first 5000 iterations discarded as burn-in and thinned the remaining samples by 1 in three parallel chains. Because we were aiming to fit a general model structure to many species' biomasses, we used vague priors to estimate all parameters (Annexe 4: Table S2) and evaluated them using prior simulations (Fig. S1 and Fig. S2). Convergence of the three chains was investigated with traceplots (Fig. S3), rank normalized split-$\hat{R}$, and effective sample sizes (Fig. S4). The smooth function for biomass through time was built with nine knots across the 33-year time series, which is equivalent to one knot every four years, to capture variation on the scale of 4 years or longer (i.e., not annual fluctuations). Adding more knots did not explain more residual variation.

The rate of change in species abundance

To estimate the annual rate of change in abundance for each species, we took the first derivative of each species' predicted biomass trend for all iterations. For each species, we took the median derivative at each time step and set a 90% credible interval around this trend as the 5% and 95% quantile of the posterior distribution of derivatives.

To estimate the average rate of change in abundance for the entire community, we took the median derivative across all species for each time step and took the 90% credible interval around this trend. All species therefore contribute equally to the community's average rate of

change through time. However, it is important to interpret these rates of change within the context that declines are most dangerous when they occur in species that represent a large portion of the community's biomass, and therefore have a larger impact on ecosystem functioning.

Long-term species associations

Associations between species' long-term trajectories are the outcomes of several years of abundance changes (i.e., not annual variability). To estimate long-term associations, we fit a linear regression to each species' biomass through time with a zero intercept to obtain a linear slope that indicates the overall magnitude and direction of abundance changes for a given species (Fig. S9). We multiplied their linear slopes to obtain pairwise long-term associations between species, where: (1) the sign indicates whether species' abundance trends were in the same direction, and (2) the magnitude indicates the severity of the species' abundance changes, where high values indicate that large abundance changes in at least one of the species. Large positive values then indicate large same-direction changes between species – that is, large absolute abundance changes – while large negative values indicate reshuffling (i.e., large opposite-direction changes).

The Living Planet Index

To calculate the Living Planet Index for the 29 Newfoundland shelf groundfish species between 1981 and 2013, we used the *rlpi* package in R[67].

Figures

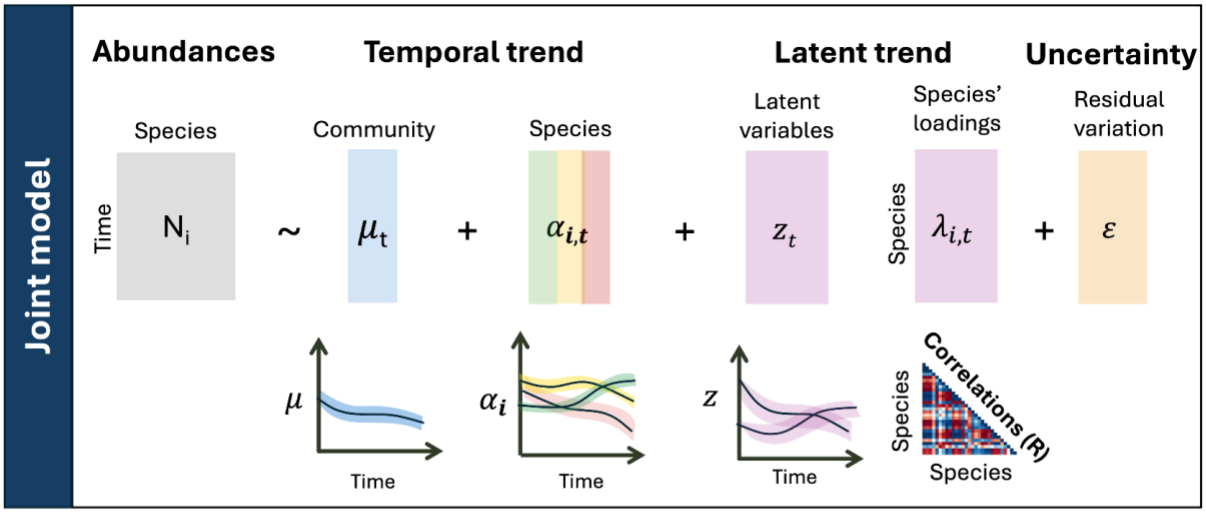
Joint model
Abundances
Temporal trend
Latent trend
Uncertainty
Species
Community
Species
Latent variables
Species' loadings
Residual variation
Time
N_i
~
μ_t
+
$\alpha_{i,t}$
+
z_t
Species
$\lambda_{i,t}$
+
ε
μ
Time
α_i
Time
z
Time
Species
Correlations (R)
Species

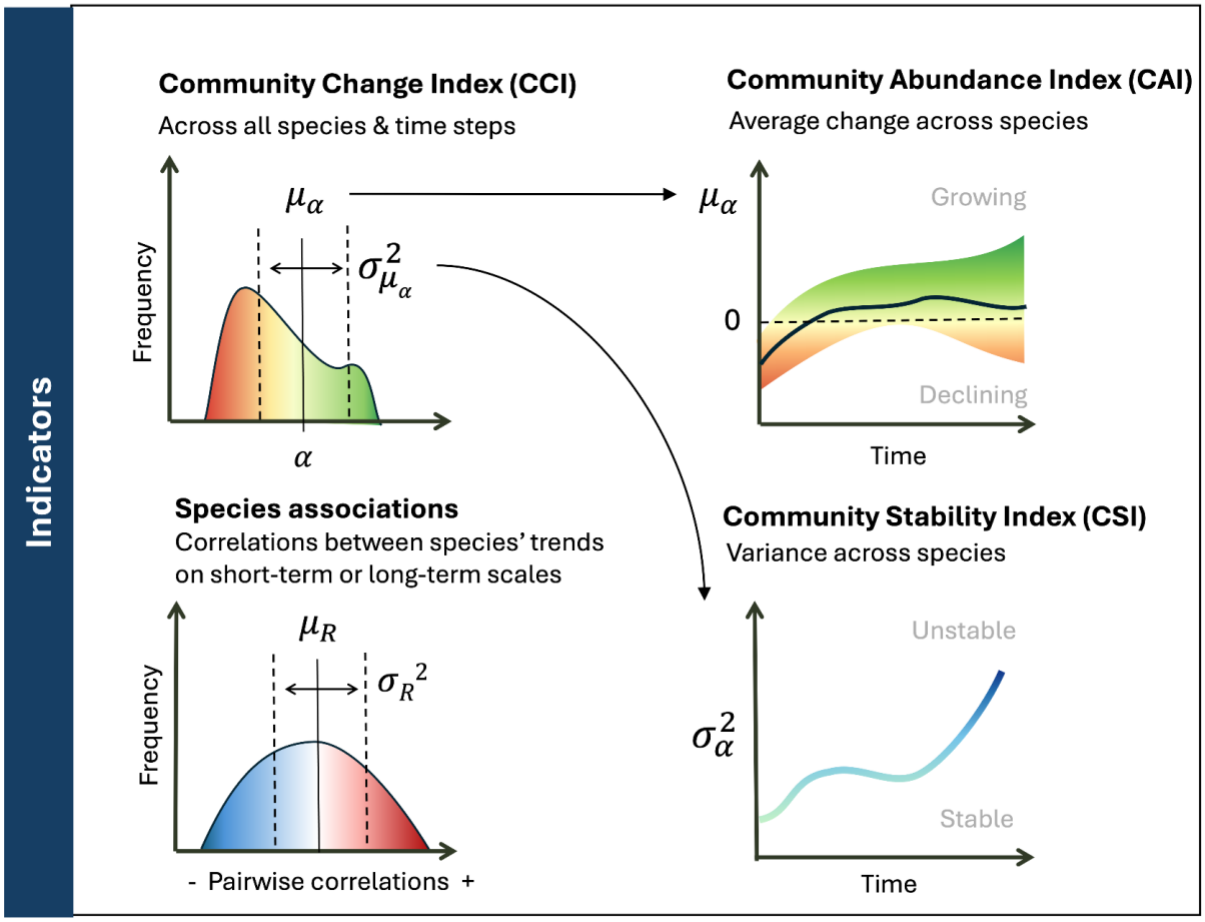
Indicators
Community Change Index (CCI)
Across all species & time steps
μ_α
$\sigma^2_{\mu_\alpha}$
Frequency
α
Community Abundance Index (CAI)
Average change across species
μ_α
Growing
0
Declining
Time
Species associations
Correlations between species' trends on short-term or long-term scales
μ_R
$\sigma_R{}^2$
Frequency
- Pairwise correlations +
Community Stability Index (CSI)
Variance across species
Unstable
σ^2_α
Stable
Time

Figure 1. Deriving biodiversity indicators from a joint species abundance model to understand the collective implications of species' trends for community stability.

The joint model estimates a temporal trend that includes a shared community-level trend and species-level trends, a latent trend that captures residual correlations between species (represented by model-generated latent variables and species' loadings), and an uncertainty component (i.e., residual variation). From this model, we derive three indicators of biodiversity change. First, the (1) Community Change Index consists of average absolute change (μ_α) and degree of reshuffling (the variance σ_α^2) which reflects change in community structure, where high variance indicates community reshuffling. This distribution is broken down into two components to track change in community structure through time: (2) the Community Abundance Index, summarising the average change in species' abundances, (3) the Community Stability Index, which summarises the diversity of trends within the community at each time step. When abundance trends are highly variable across species, community structure is reorganized, and ecosystem function is likely to change. The species associations can then be interpreted across time scales. At short time scales, they describe how fluctuations propagate through the community, with positive correlations indicating synchronized dynamics that amplify variability while negative or weak correlations reflect compensatory dynamics that buffer it. Over longer time scales, these associations capture how species' trajectories are coupled; strong positive correlations indicate coordinated trends across species, whereas weak or negative correlations indicate divergence in trajectories and reorganization of community structure. When positively correlated trends are associated with widespread declines, they reveal synchronized declines that can threaten community stability.

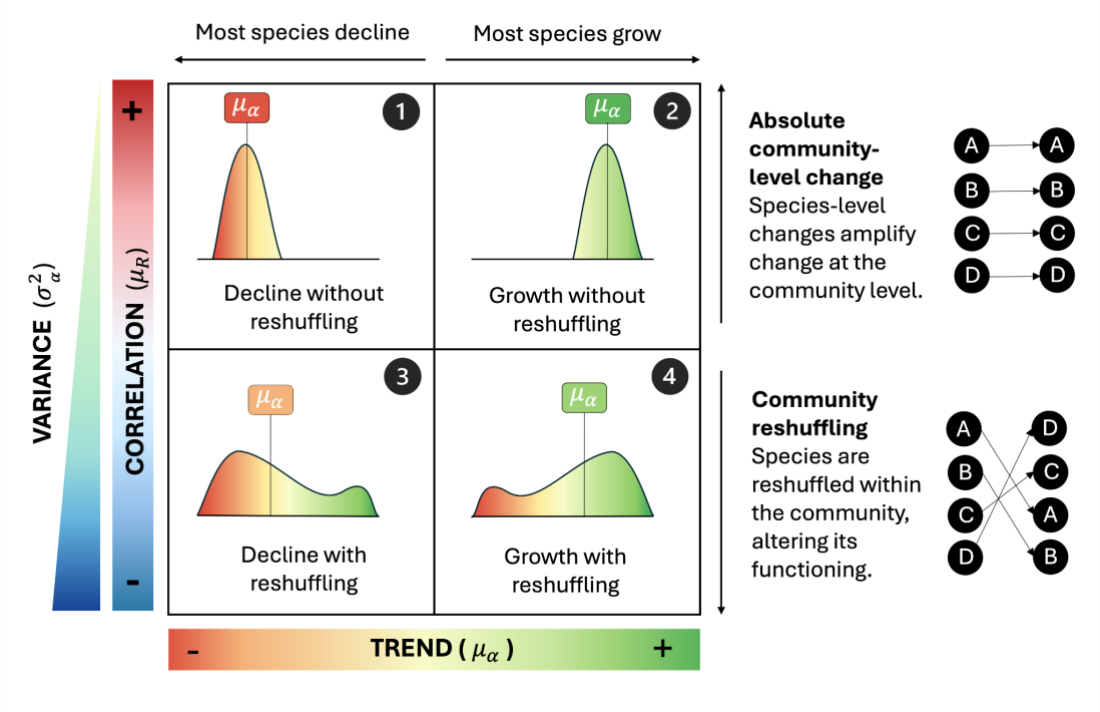

Figure 2. How the community indicators collectively summarise change in community abundance and structure.

Each panel shows a distribution of species' trends over a given time frame, which is typically summarised as an average (μ_α) to represent the community-level change in abundance. But an average is only part of the picture – the variance and correlation between species' trends determines how species-level changes scale up to impact the community. In the top row, species show similar trends (i.e., positively correlated and low-variance), and therefore combine to amplify absolute community-level change (i.e., total community biomass). In the bottom row, species trends vary widely (and species pairs are negatively correlated), which indicates community reshuffling – where there is a higher risk of changing *community functioning* despite not necessarily detecting large absolute change at the community scale. Even in cases where community-level average is low or positive (right column), high variance between species' trends can fundamentally change the community.

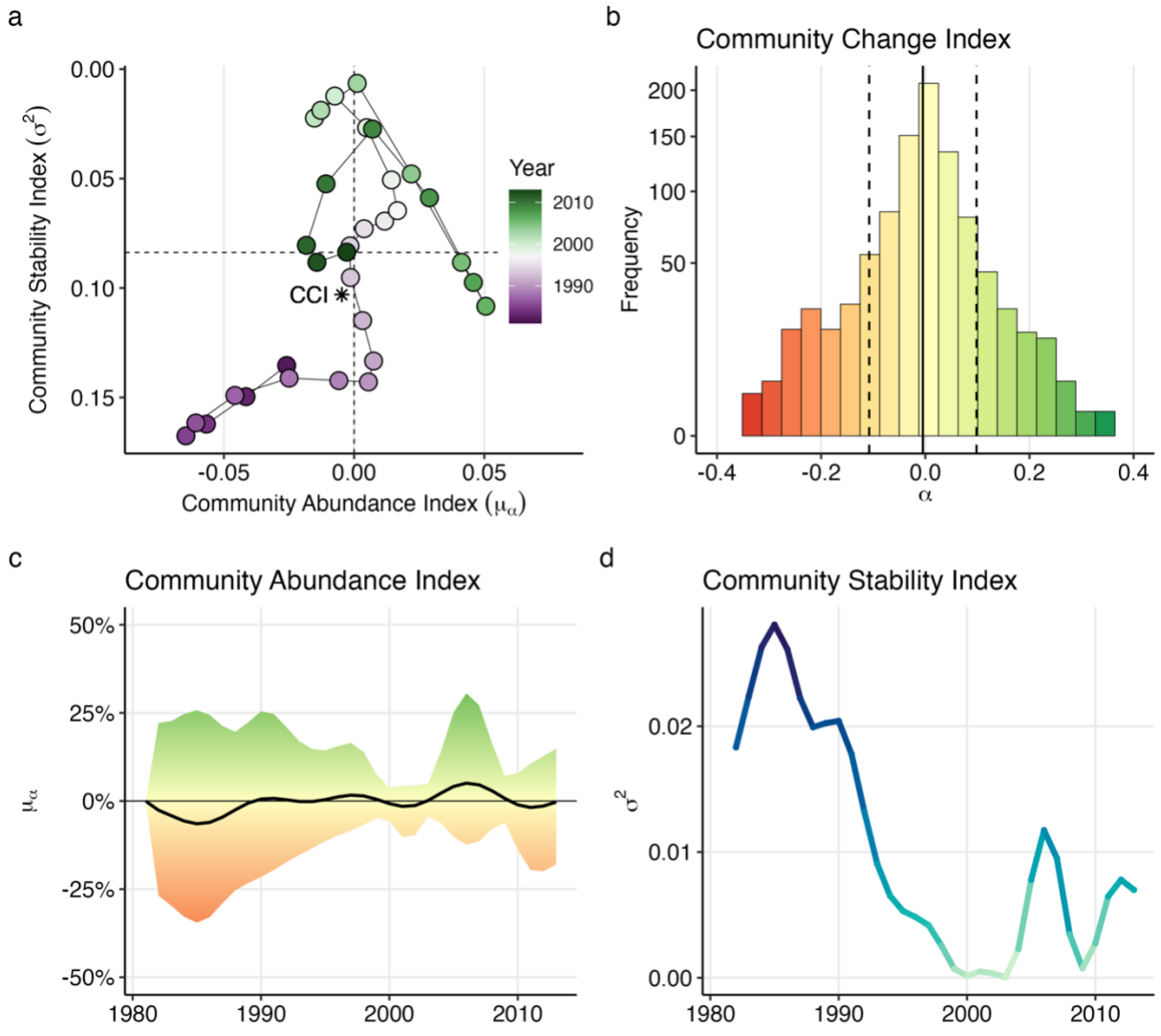

Figure 3. Indices of community change summarise the collapse and early recovery of the Newfoundland shelf groundfish community between 1981 and 2013.

(a) Trajectory of community dynamics through time, summarizing the three indices. Quadrants correspond to Fig. 2, where the center represents the community's average CAI and CSI scores. The trajectory illustrates the community's changing dynamics from widespread declines with community reshuffling (bottom-right) towards early signs of slow recovery (top panels). (b) Community Change Index (CCI): The distribution of annual rates of change in biomass for all

species in the community between 1981 and 2013. The mean rate of change across all species is shown as the solid line, and the dotted lines show the standard deviation around the mean (μ_α = -0.3%, SD = 0.11). (c) Community Abundance Index (CAI): The community's average trend in the rate of change in biomass over the entire period, with a 90% credible interval that is shaded to show the range of rates of change that are included within the interval. (d) Community Stability Index (CSI): The variability through time shown as the annual variability across species within the community measured as the standard deviation of rates of change across all species each year.

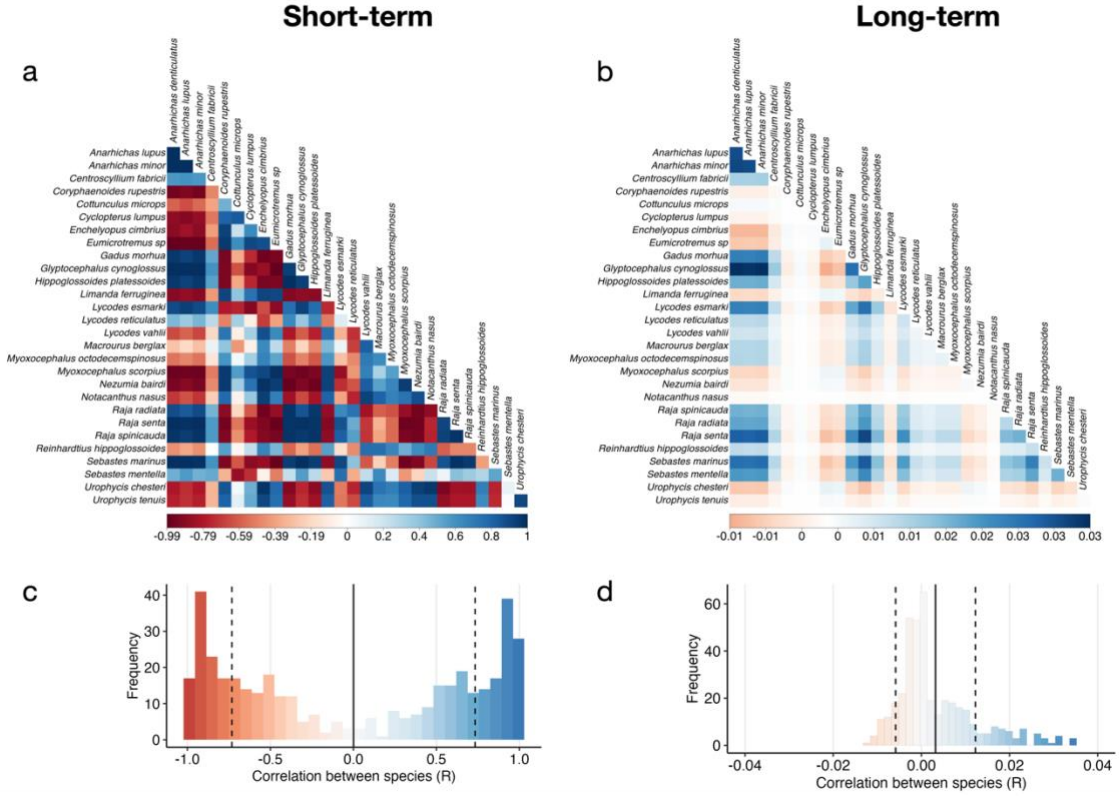

Figure 4. Unpacking community dynamics from short-term and long-term species associations in the Newfoundland shelf groundfish community between 1981 and 2013.

Short-term correlations between species' biomass trends are shown in panels (a) and (c), and long-term correlations between species' linear changes in biomass are shown in panels (b) and (d). (a) Average residual correlations between species' biomass annual variations over the entire period. (b) Long-term correlations between species' overall biomass trends from 1981 to 2013, measured as the multiplied linear slopes of each species pair. The distribution of (c) the short-term correlations between species' annual biomass fluctuations (mean = 0.00074, SD = 0.73) and (d) long-term correlations between species' linear trend in biomasses (mean = 0.0032, SD = 0.0091). The mean correlation between species is shown as the solid line, and the dotted lines show the standard deviation around the mean.

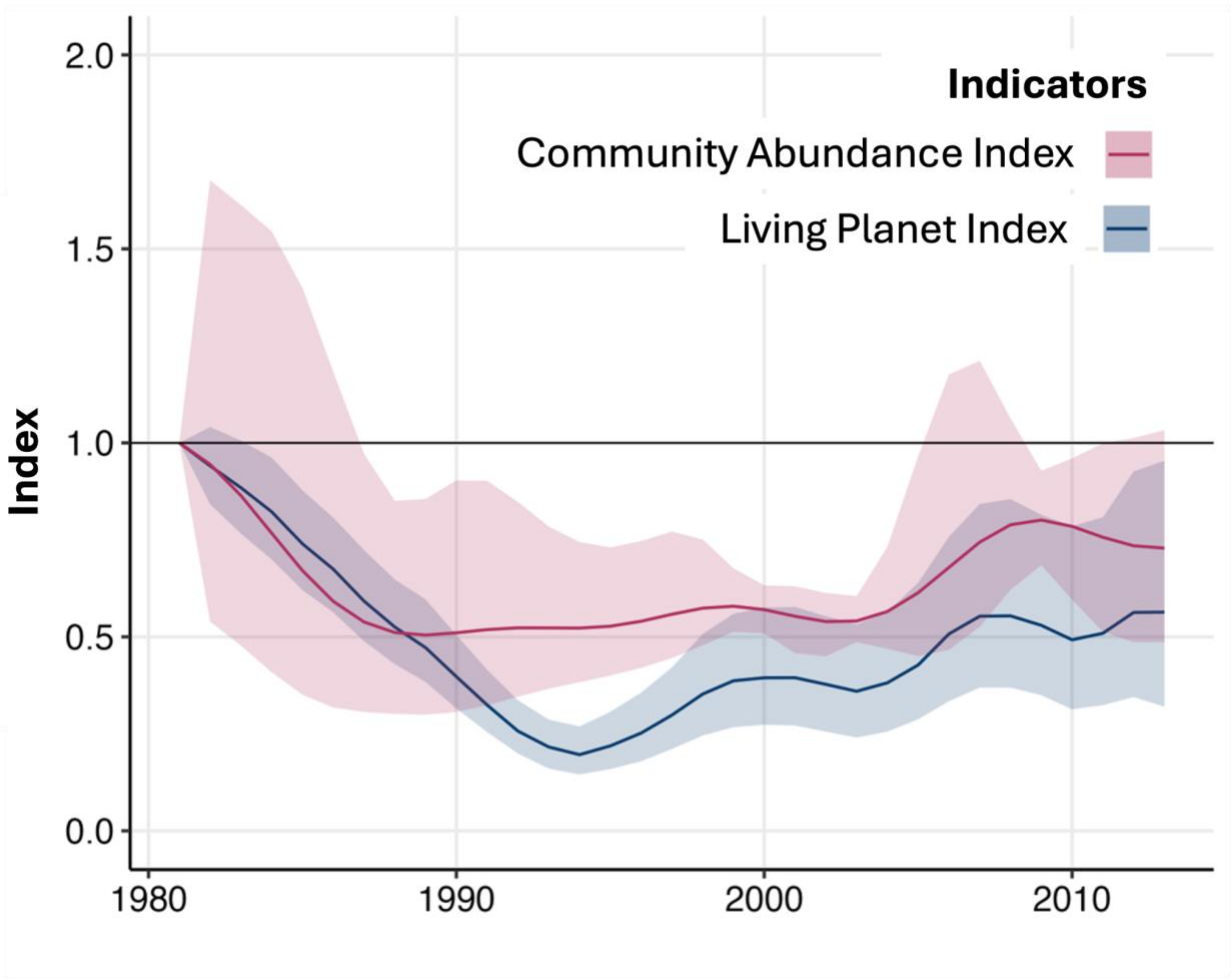

Figure 5. Comparing the Community Abundance Index (CAI) to the Living Planet Index (LPI) for the Newfoundland shelf groundfish community between 1981 and 2013.

The Living Planet Index (in blue) measures the average change in relative abundance (here, measured as the biomass in kg/tow) of species compared to a baseline of 1, set in 1981. The blue ribbon shows the 95% confidence intervals around the LPI. The Community Abundance Indicator (in red) shows the average growth rate from the posterior distribution of predicted biomass trends from the joint abundance model, compared to a baseline of 1. The red ribbon shows the 95% credible interval of the CAI (i.e., the estimated growth rates derived from the posterior distribution of predicted trends).

References

1. McKinney, M.L., and Lockwood, J.L. (1999). Biotic homogenization: a few winners replacing many losers in the next mass extinction. Trends Ecol. Evol. *14*, 450–453.
2. Dornelas, M., Gotelli, N.J., Shimadzu, H., Moyes, F., Magurran, A.E., and McGill, B.J. (2019). A balance of winners and losers in the Anthropocene. Ecol. Lett. *22*, 847–854.
3. Ives, A.R. (1995). Predicting the Response of Populations to Environmental Change. Ecology *76*, 926–941.
4. Elmqvist, T., Folke, C., Nyström, M., Peterson, G., Bengtsson, J., Walker, B., and Norberg, J. (2003). Response diversity, ecosystem change, and resilience. Front. Ecol. Environ. *1*, 488–494.
5. Estes, J.A., Terborgh, J.W., Brashares, J., Power, M.E., Berger, J., Bond, W.J., Carpenter, S., and Wardle, D. (2011). Trophic Downgrading of Planet Earth. Science *215*, 1501–1503.
6. Brodie, J.F., Aslan, C.E., Rogers, H.S., Redford, K.H., Maron, J.L., Bronstein, J.L., and Groves, C.R. (2014). Secondary extinctions of biodiversity. Trends Ecol. Evol. *29*, 664–672.
7. Belitz, M.W., Campbell, C.J., Drum, R.G., Leuenberger, W., Morelli, T.L., Nail, K., Shirey, V., Thogmartin, W., and Zipkin, E.F. (2025). A case for assemblage-level conservation to address the biodiversity crisis. Nat. Rev. Biodivers., 1–10.
8. Tobias, J.A., Bullock, J.M., Dicks, L.V., Forester, B.R., and Razgour, O. (2025). Biodiversity conservation requires integration of species-centric and process-based strategies. Proc. Natl. Acad. Sci. *122*, e2410936122.
9. Dornelas, M., Gotelli, N.J., McGill, B., Shimadzu, H., Moyes, F., Sievers, C., and Magurran, A.E. (2014). Assemblage time series reveal biodiversity change but not systematic loss. Science *344*, 296–299.
10. Trisos, C.H., Merow, C., and Pigot, A.L. (2020). The projected timing of abrupt ecological disruption from climate change. Nature *580*, 496–501.
11. Ledger, S.E.H., Loh, J., Almond, R., Böhm, M., Clements, C.F., Currie, J., Deinet, S., Galewski, T., Grooten, M., Jenkins, M., et al. (2023). Past, present, and future of the Living Planet Index. Npj Biodivers. *2*, 1–13.
12. Loh, J., Green, R.E., Ricketts, T., Lamoreux, J., Jenkins, M., Kapos, V., and Randers, J. (2005). The Living Planet Index: Using species population time series to track trends in biodiversity. Philos. Trans. R. Soc. B Biol. Sci. *360*, 289–295.
13. Haynes, K.J., Liebhold, A.M., Fearer, T.M., Wang, G., Norman, G.W., and Johnson, D.M. (2009). Spatial synchrony propagates through a forest food web via consumer-resource interactions. Ecology *90*, 2974–2983.
14. Jarillo, J., Sæther, B.-E., Engen, S., and Cao-García, F.J. (2020). Spatial Scales of Population Synchrony in Predator-Prey Systems. Am. Nat. *195*, 216–230.
15. Lertzman-Lepofsky, G., Dolezal, A.J., Waters, M.T., Fuster-Calvo, A., Black, E.N., Flaman, S., Straus, S., Langendorf, R.E., Eckert, I., Fan, S., et al. Temporal changes in

taxon abundances are positively correlated but poorly predicted at the global scale. Ecography, e07195.
16. Bjørnstad, O.N., Ims, R.A., and Lambin, X. (1999). Spatial population dynamics: analyzing patterns and processes of population synchrony. Trends Ecol. Evol. *14*, 427–432.
17. Hansen, B.B., Grøtan, V., Herfindal, I., and Lee, A.M. (2020). The Moran effect revisited: spatial population synchrony under global warming. Ecography *43*, 1591–1602.
18. Johnson, T.F., Beckerman, A.P., Childs, D.Z., Webb, T.J., Evans, K.L., Griffiths, C.A., Capdevila, P., Clements, C.F., Besson, M., Gregory, R.D., et al. (2024). Revealing uncertainty in the status of biodiversity change. Nature, 1–7.
19. Hébert, K., and Gravel, D. (2023). The Living Planet Index's ability to capture biodiversity change from uncertain data. Ecology *104*, e4044.
20. Pimm, S.L., Jones, H.L., and Diamond, J. (1988). On the Risk of Extinction. Am. Nat. *132*, 757–785.
21. Melbourne, B.A., and Hastings, A. (2008). Extinction risk depends strongly on factors contributing to stochasticity. Nature *454*, 100–103.
22. Collen, B., Mcrae, L., Deinet, S., de Palma, A., Carranza, T., Cooper, N., Loh, J., and Baillie, J.E.M. (2011). Predicting how populations decline to extinction. Philos. Trans. R. Soc. B Biol. Sci. *366*, 2577–2586.
23. Palmqvist, E., and Lundberg, P. (1998). Population Extinctions in Correlated Environments. Oikos *83*, 359–367.
24. Schindler, D.E., Armstrong, J.B., and Reed, T.E. (2015). The portfolio concept in ecology and evolution. Front. Ecol. Environ. *13*, 257–263.
25. Gonzalez, A., and Loreau, M. (2009). The Causes and Consequences of Compensatory Dynamics in Ecological Communities. Annu. Rev. Ecol. Evol. Syst. *40*, 393–414.
26. Shoemaker, L.G., Hallett, L.M., Zhao, L., Reuman, D.C., Wang, S., Cottingham, K.L., Hobbs, R.J., Castorani, M.C.N., Downing, A.L., Dudney, J.C., et al. (2022). The long and the short of it: Mechanisms of synchronous and compensatory dynamics across temporal scales. Ecology *103*, e3650.
27. Polazzo, F., Limberger, R., Pennekamp, F., Ross, S.R.P.-J., Simpson, G.L., and Petchey, O.L. (2024). Measuring the Response Diversity of Ecological Communities Experiencing Multifarious Environmental Change. Glob. Change Biol. *30*, e17594.
28. Fuster-Calvo, A., Higino, G.T., Parent, C., Caron, D., Banville, F., Massol, F., Blanchet, F.G., Hébert, K., Pollock, L., Maiorano, L., et al. (2025). Tracking community change via network coherence. Preprint at bioRxiv, https://doi.org/10.1101/2025.11.04.686602.
29. Wang, J., Grimm, N.B., Lawler, S.P., and Dong, X. (2023). Changing climate and reorganized species interactions modify community responses to climate variability. Proc. Natl. Acad. Sci. *120*, e2218501120.

30. Kindsvater, H.K., Dulvy, N.K., Horswill, C., Juan-Jordá, M.-J., Mangel, M., and Matthiopoulos, J. (2018). Overcoming the Data Crisis in Biodiversity Conservation. Trends Ecol. Evol. *33(9)*, 676-688.
31. Sharma, S., Winner, K., Pollock, L.J., Thorson, J.T., Mäkinen, J., Merow, C., Pedersen, E.J., Chefira, K.F., Portmann, J.M., Iannarilli, F., et al. (2025). No species left behind: borrowing strength to map data-deficient species. Trends Ecol. Evol. *40*, 699–711.
32. Ovaskainen, O., Ramos, D.L., Slade, E.M., Merckx, T., Tikhonov, G., Pennanen, J., Pizo, M.A., Ribeiro, M.C., and Morales, J.M. (2019). Joint species movement modeling: how do traits influence movements? Ecology, e02622.
33. Pollock, L.J., Tingley, R., Morris, W.K., Golding, N., O'Hara, R.B., Parris, K.M., Vesk, P.A., and McCarthy, M.A. (2014). Understanding co-occurrence by modelling species simultaneously with a Joint Species Distribution Model (JSDM). Methods Ecol. Evol. *5*, 397–406.
34. Poggiato, G., Münkemüller, T., Bystrova, D., Arbel, J., Clark, J.S., and Thuiller, W. (2021). On the Interpretations of Joint Modeling in Community Ecology. Trends Ecol. Evol. *36*, 391–401.
35. Ovaskainen, O., Tikhonov, G., Norberg, A., Guillaume Blanchet, F., Duan, L., Dunson, D., Roslin, T., and Abrego, N. (2017). How to make more out of community data? A conceptual framework and its implementation as models and software. Ecol. Lett. *20*, 561–576.
36. Smith, A.C., Binley, A.D., Daly, L., Edwards, B.P.M., Ethier, D., Frei, B., Iles, D., Meehan, T.D., Michel, N.L., and Smith, P.A. (2023). Spatially explicit Bayesian hierarchical models improve estimates of avian population status and trends. Ornithol. Appl., duad056.
37. Clark, N.J., and Wells, K. (2022). Dynamic generalised additive models (DGAMs) for forecasting discrete ecological time series. Methods Ecol. Evol. *00*, 1–14.
38. Clark, N.J., Ernest, S.K.M., Senyondo, H., Simonis, J., White, E.P., Yenni, G.M., and Karunarathna, K. a. N.K. (2025). Beyond single-species models: leveraging multispecies forecasts to navigate the dynamics of ecological predictability. PeerJ *13*, e18929.
39. Tikhonov, G., Abrego, N., Dunson, D., and Ovaskainen, O. (2017). Using joint species distribution models for evaluating how species-to-species associations depend on the environmental context. Methods Ecol. Evol. *8*, 443–452.
40. Warton, D.I., Blanchet, F.G., O'Hara, R.B., Ovaskainen, O., Taskinen, S., Walker, S.C., and Hui, F.K.C. (2015). So Many Variables: Joint Modeling in Community Ecology. Trends Ecol. Evol. *30*, 766–779.
41. Rigal, S., and Knape, J. (2023). A toolbox to explore the composition of species dynamics behind multi-species indices. Methods Ecol. Evol. *14*, 1821–1832.
42. May, R.M. (1973). Stability and Complexity in Model Ecosystems (Princeton University Press).

43. Lundberg, P., Ranta, E., Ripa, J., and Kaitala, V. (2000). Population variability in space and time. Trends Ecol. Evol. *15*, 460–464.
44. Bjørnstad, O.N., and Grenfell, B.T. (2001). Noisy Clockwork: Time Series Analysis of Population Fluctuations in Animals. Science *293*, 638–643.
45. Hovestadt, T., and Nowicki, P. (2008). Process and measurement errors of population size: their mutual effects on precision and bias of estimates for demographic parameters. Biodivers. Conserv. *17*, 3417–3429.
46. Pedersen, E.J., Koen-Alonso, M., and Tunney, T.D. (2020). Detecting regime shifts in communities using estimated rates of change. ICES J. Mar. Sci. *77*, 1546–1555.
47. Pedersen, E.J., Thompson, P.L., Ball, R.A., Fortin, M.J., Gouhier, T.C., Link, H., Moritz, C., Nenzen, H., Stanley, R.R.E., Taranu, Z.E., et al. (2017). Signatures of the collapse and incipient recovery of an overexploited marine ecosystem. R. Soc. Open Sci. *4*.
48. Hutchings, J.A., and Reynolds, J.D. (2004). Marine Fish Population Collapses: Consequences for Recovery and Extinction Risk. BioScience *54*, 297–309.
49. COSEWIC (2003). Atlantic Cod (Gadus morhua) (COSEWIC).
50. Hanson, J.M., and Chouinard, G.A. (2002). Diet of Atlantic cod in the southern Gulf of St Lawrence as an index of ecosystem change. J. Fish Biol. *60*, 902–922.
51. COSEWIC (2010). Assessment and update status report on the Atlantic Cod (Gadus morhua).
52. Benoît, H.P., Swain, D.P., Bowen, W.D., Breed, G.A., Hammill, M.O., and Harvey, V. (2011). Evaluating the potential for grey seal predation to explain elevated natural mortality in three fish species in the southern Gulf of St. Lawrence. Mar. Ecol. Prog. Ser. *442*, 149–167.
53. Bousquet, N., Chassot, E., Duplisea, D.E., and Hammill, M.O. (2014). Forecasting the Major Influences of Predation and Environment on Cod Recovery in the Northern Gulf of St. Lawrence. PLOS ONE *9*, e82836.
54. Benedetti-Cecchi, L., Bates, A.E., Strona, G., Bulleri, F., Horta e Costa, B., Edgar, G.J., Hereu, B., Reed, D.C., Stuart-Smith, R.D., Barrett, N.S., et al. (2024). Marine protected areas promote stability of reef fish communities under climate warming. Nat. Commun. *15*, 1822.
55. Fischhoff, B., and Davis, A.L. (2014). Communicating scientific uncertainty. Proc. Natl. Acad. Sci. *111*, 13664–13671.
56. Rowland, J.A., Bland, L.M., James, S., and Nicholson, E. (2021). A guide to representing variability and uncertainty in biodiversity indicators. Conserv. Biol. *35*, 1669–1682.
57. Leung, B., and Gonzalez, A. (2024). Global monitoring for biodiversity: Uncertainty, risk, and power analyses to support trend change detection. Sci. Adv. *10*, eadj1448.
58. Cressie, N., Calder, C.A., Clark, J.S., Ver Hoef, J.M., and Wikle, C.K. (2009). Accounting for uncertainty in ecological analysis: The strengths and limitations of hierarchical statistical modeling. Ecol. Appl. *19*, 553–570.

59. Puurtinen, M., Elo, M., and Kotiaho, J.S. (2022). The Living Planet Index does not measure abundance. Nature *601*, E14–E15.
60. Kissling, W.D., Ahumada, J.A., Bowser, A., Fernandez, M., Fernández, N., García, E.A., Guralnick, R.P., Isaac, N.J.B., Kelling, S., Los, W., et al. (2018). Building essential biodiversity variables (EBVs) of species distribution and abundance at a global scale. Biol. Rev. *93*, 600–625.
61. Schmeller, D.S., Weatherdon, L.V., Loyau, A., Bondeau, A., Brotons, L., Brummitt, N., Geijzendorffer, I.R., Haase, P., Kuemmerlen, M., Martin, C.S., et al. (2018). A suite of essential biodiversity variables for detecting critical biodiversity change. Biol. Rev. *93*, 55–71.
62. Dornelas, M., Antão, L.H., Moyes, F., Bates, A.E., Magurran, A.E., Adam, D., Akhmetzhanova, A.A., Appeltans, W., Arcos, J.M., Arnold, H., et al. (2018). BioTIME: A database of biodiversity time series for the Anthropocene. Glob. Ecol. Biogeogr. *27*, 760–786.
63. Gonzalez, A., Chase, J.M., and O'Connor, M.I. (2023). A framework for the detection and attribution of biodiversity change. Philos. Trans. R. Soc. B Biol. Sci. *378*, 20220182.
64. CBD (2022). 15/4. Kunming-Montreal Global Biodiversity Framework.
65. Hébert, K., Acevedo, D.H., Cameron, V., Courant, S., Daguet, C., Gonzalez, A., Gravel, D., Huot, J., Jousse, M., Juhasz, C.-C., et al. (2025). Selecting indicators to track progress towards the Global Biodiversity Framework: a case study of Quebec's 2030 Nature Plan. FACETS *10*, 1–13.
66. Thorson, J.T., Ianelli, J.N., Larsen, E.A., Ries, L., Scheuerell, M.D., Szuwalski, C., and Zipkin, E.F. (2016). Joint dynamic species distribution models: a tool for community ordination and spatio-temporal monitoring. Glob. Ecol. Biogeogr. *25*, 1144–1158.
67. Freeman, R., McRae, L., Deinet, S., Amin, R., and Collen, B. (2022). rlpi: Tools for calculating indices using the Living Planet Index method.
68. Colbourne, E., Holden, J., Snook, S., Han, G., Lewis, S., Senciall, D., Bailey, W., Higdon, J., and Chen, N. (2017). Physical oceanographic conditions on the Newfoundland and Labrador Shelf during 2016. Can. Sci. Advis. Secr. CSAS. man, R., McRae, L., Deinet, S., Amin, R., and Collen, B. (2022). rlpi: Tools for calculating indices using the Living Planet Index method.

SUPPLEMENTARY INFORMATION

1. RELATING LATENT TRENDS TO POTENTIAL DRIVERS OF CHANGE

Latent variables may be helpful to generate hypotheses about drivers of change that can then be more formally investigated to attribute detected changes to their causes. In this system, the two latent variables generated by the model were strongly correlated with overexploitation and climate variations (Fig. S1.1), which are the two principal drivers of the abundance changes in this groundfish community between 1981 and 2013 (Pedersen et al. 2017). The first latent variable was highly correlated (Pearson $R = 0.95$, $p < 0.001$) with the smoothed total annual catch in fishing vessels targeting benthic fish in NAFO divisions 2J, 3K and 3L (Pedersen et al. 2017). The second latent variable was highly correlated (Pearson $R = 0.85$, $p < 0.001$) with a smoothed version of a composite climate index calculated for this region, representing several climate variables known to influence the groundfish community (Pedersen et al. 2017). Though correlation does not imply causality, the similarities between latent variables and known drivers of change in this system highlight the potential for hypothesis generation in other systems.

Exploring species' estimated loadings for each of the two latent variables can then further help to generate hypotheses about the drivers of species' trends (Fig. S1.2) (see Rigal & Knape 2023).

Methods

To demonstrate the potential for using latent trend modelling as a potential avenue to build hypotheses for change attribution, we compared the two model-generated latent variables with two drivers of change in this system, which were not included as predictors in the model. In this system, overexploitation and climate variations were the two principal drivers of the abundance changes in this groundfish community between 1981 and 2013 (Pedersen et al. 2017).

To investigate overexploitation, we used the total catch per year by fishing vessels in the NAFO divisions 2 J, 3 K and 3 L from ships recorded as targeting benthic fish, as calculated by Pedersen et al. (2017) (series 21B; www.nafo.int/Data/Catch-Statistics). To smooth short-term variations in catch into a more representative long-term trend, we applied a Generalized Additive Model (GAM) to the total annual catch from 1981 to 2013 (using 4 knots), then calculated the Pearson correlation between predicted annual catch (after smoothing) and Latent variable 1.

To investigate climate variability, we used a composite climate index from Pedersen et al. (2017), which takes a 5-year moving window average of the sum of several scaled environmental time series, including the North Atlantic Oscillation, ice cover and bottom and surface temperatures (as calculated for the Canadian Science Advisory Secretariat[68]). We applied a Generalized Additive Model (GAM) to this composite climate index from 1981 to 2013 (using 4 knots) to obtain a smoother long-term trend, then calculated the Pearson correlation between the smoothed climate index and Latent variable 2.

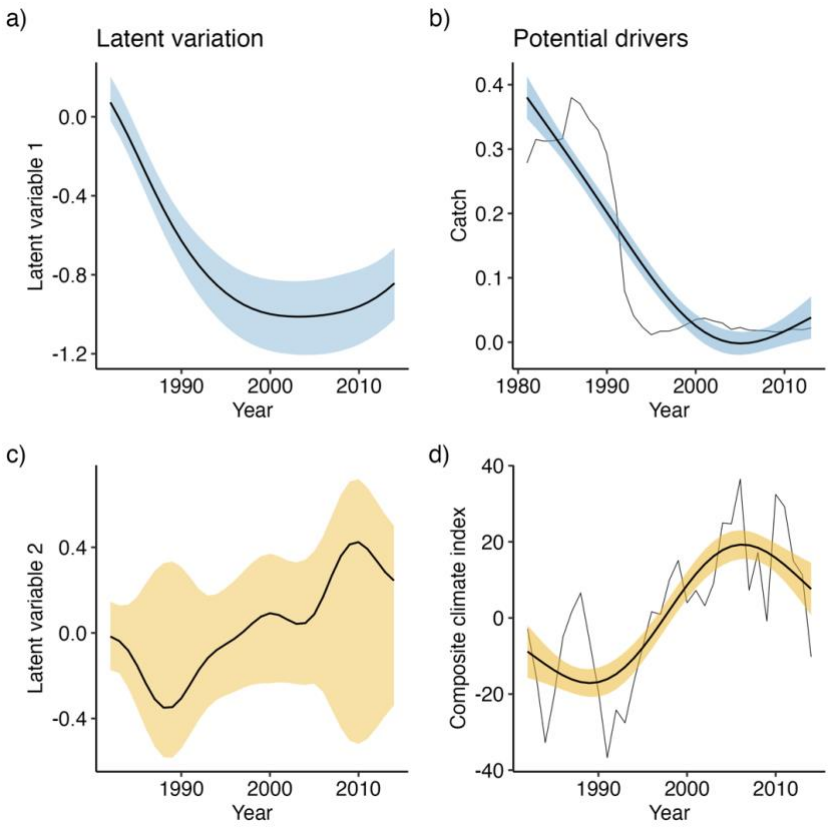

Figure S1.1. Potential for hypothesis generation for biodiversity change attribution to potential drivers from latent factors.

Latent variables 1 (a) and 2 (b) generated by the model capture latent variation in species' abundances through time, representing unmeasured predictors of species' trends. We found strong correlations between these latent variables and two drivers of change in this groundfish community between 1981 and 2013: (b) fishing pressure, measured as the total annual catch in this region, and (d) climate variability, measured as a composite climate index that was developed for this community. Panels (a) and (c) show the median trend of the latent variables with 90% credible intervals. Panels (b) and (d) show the raw values of the potential drivers of change as a thin solid line, overlayed with their long-term predicted trend (GAM with 4 knots), with the model's standard error shown as a ribbon.

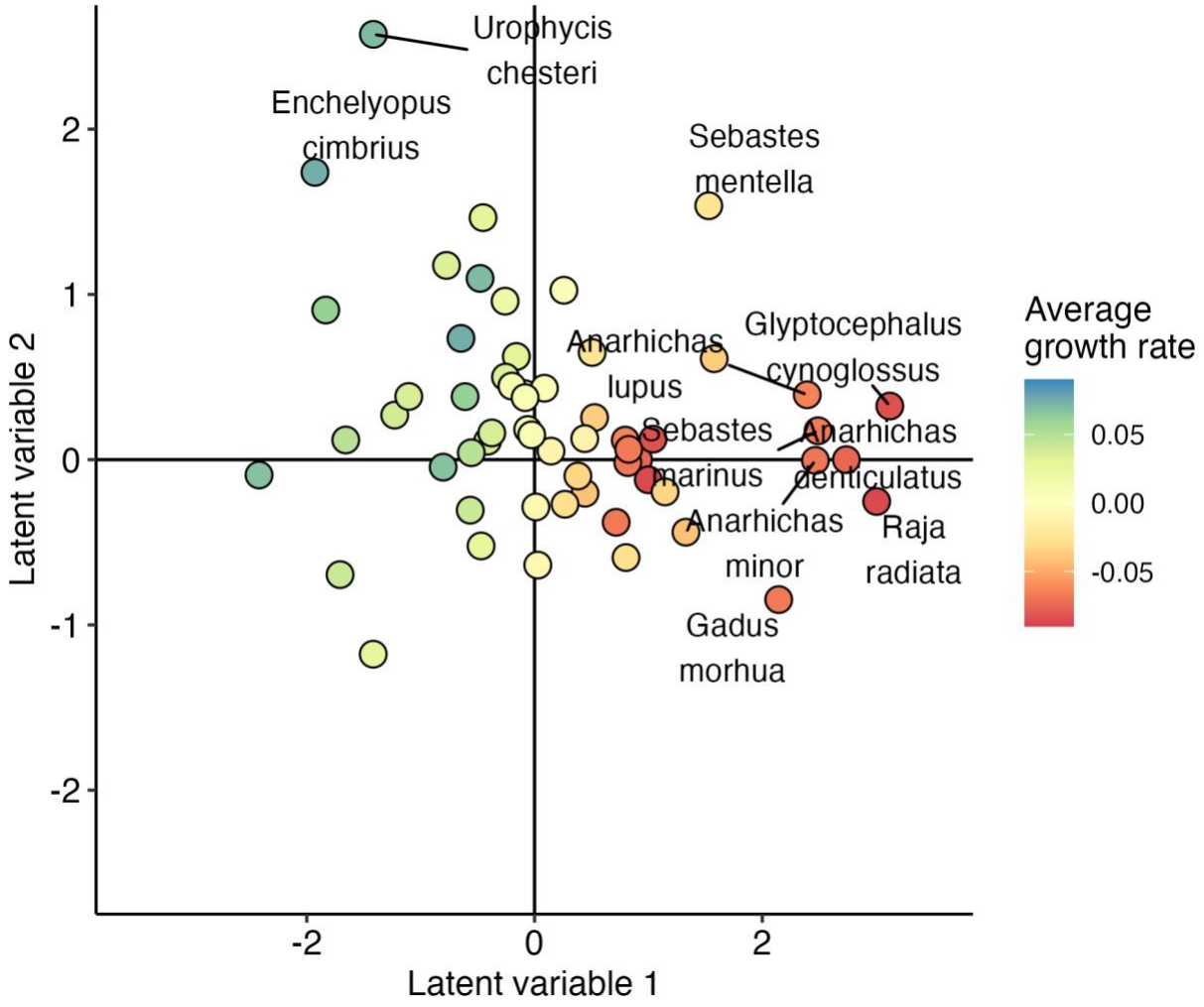

Figure S1.2. Biplot of species' factor loadings for the two latent variables included in the joint model, coloured by their average growth rate from 1981 to 2013.

Species responses to the two latent factors (Fig. S1.1) reveal species groupings according to their sensitivity to latent factors to further unpack species dynamics within the community (as in Rigal & Knape 2023). For example, species like *G. morhua*, *R. radiata*, *S. marinus*, *A. denticulatus* which suffered severe declines from overfishing responded most strongly to Latent variable 1, which exhibits a similar pattern to fishing pressure (Fig. S1.1b), measured as the total annual catch in this region.

TABLE S1. Vague priors used to estimate model parameters.

Parameter	Parameter length	Parameter description	Prior
lambda	2	s(time) smooth parameters	N(10, 25)
mu_raw	1	Random effect mean for s(series)	N(0,1)
sigma_raw	1	Random effect variance for s(series)	exp(0.5)
alpha_gp	29	Gaussian process trend amplitude	N(0, 0.5);
num_gp_basis	1	Basis dimension for approximate Gaussian process	min(20, n)
sigma_obs	29	Observation error (standard deviation)	T(3, 0, 2)

Parameter indicates the parameter name in the Stan code for the model. Parameter length indicates the number of parameter values that were estimated. Parameter description describes the parameter's role in the model. Prior indicates the prior distribution used to estimate each parameter. These priors are the default settings in the R package *mvgam*, and were kept after inspecting prior simulations.

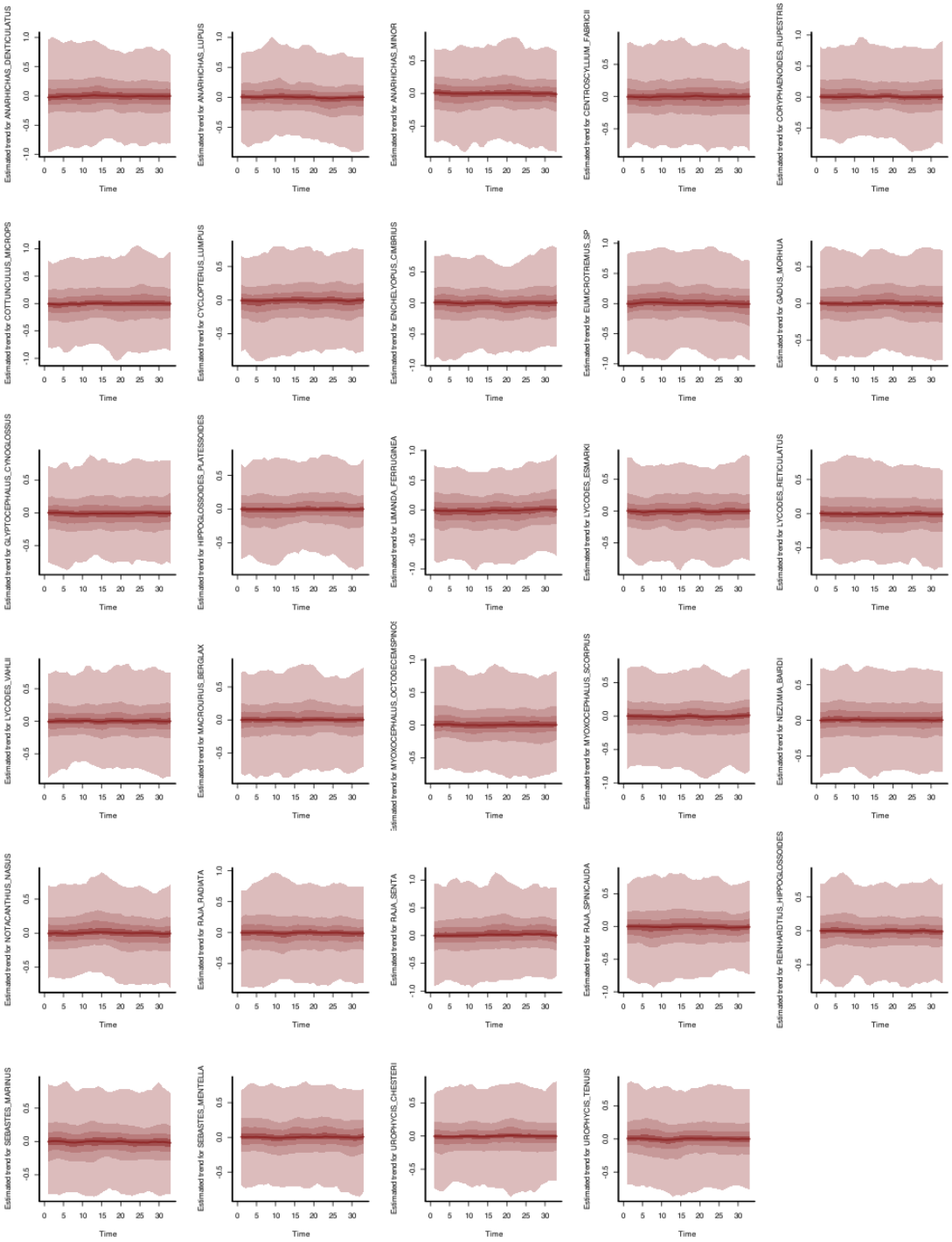

Figure S1. Prior simulations of each population's biomass trend through time.

These simulations are based on vague priors that were used to estimate all parameters, described in Annexe 4: Table S2.

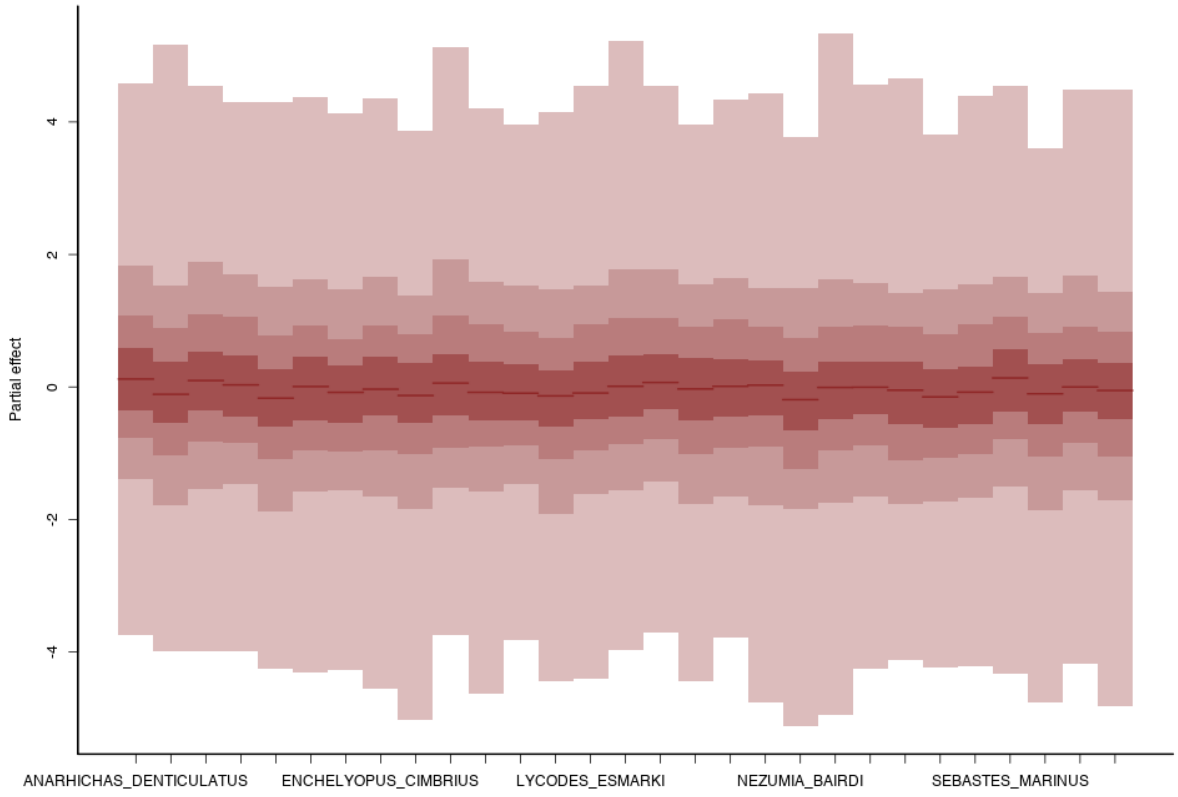

Figure S2. Prior simulations of the partial effect of each species on the temporal trend of biomass.

These simulations are based on vague priors that were used to estimate all parameters, described in Annexe 4: Table S2.

Figure S3. Trace plots for the estimated beta parameters in the Dynamic Generalized Additive Model (DGAM).

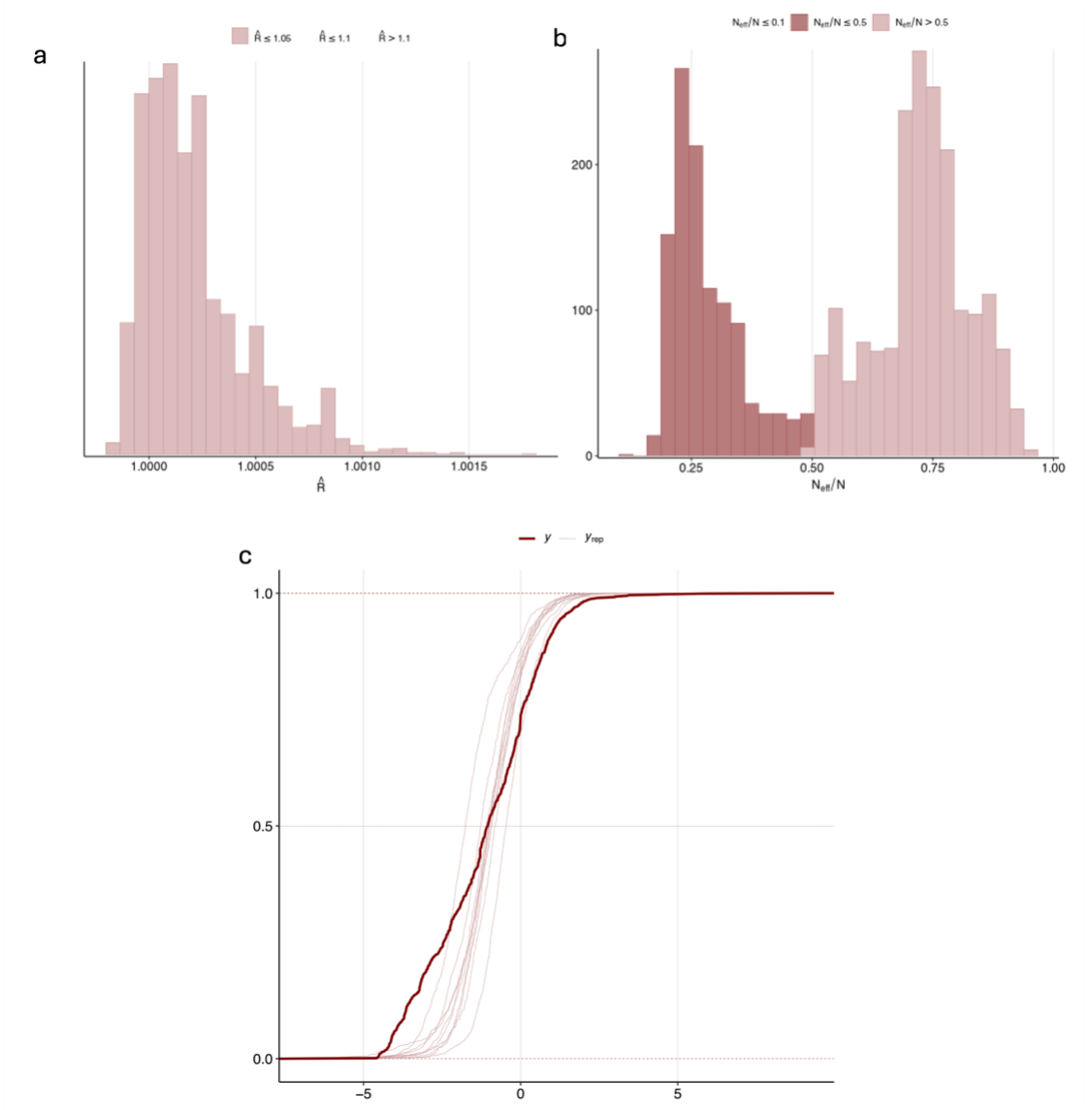

Figure S4. Model diagnostic plots.

Markov Chain Monte Carlo (MCMC) convergence diagnostics shown in (a) Histogram of Rhat convergence diagnostic and (b) Histogram of the ratios of effective sample size to total sample size. Values are colored according to default chosen thresholds (where lighter colours are better). Posterior predictive checking with the (c) ECDF (Empirical Cumulative Distribution Function) overlay plot.

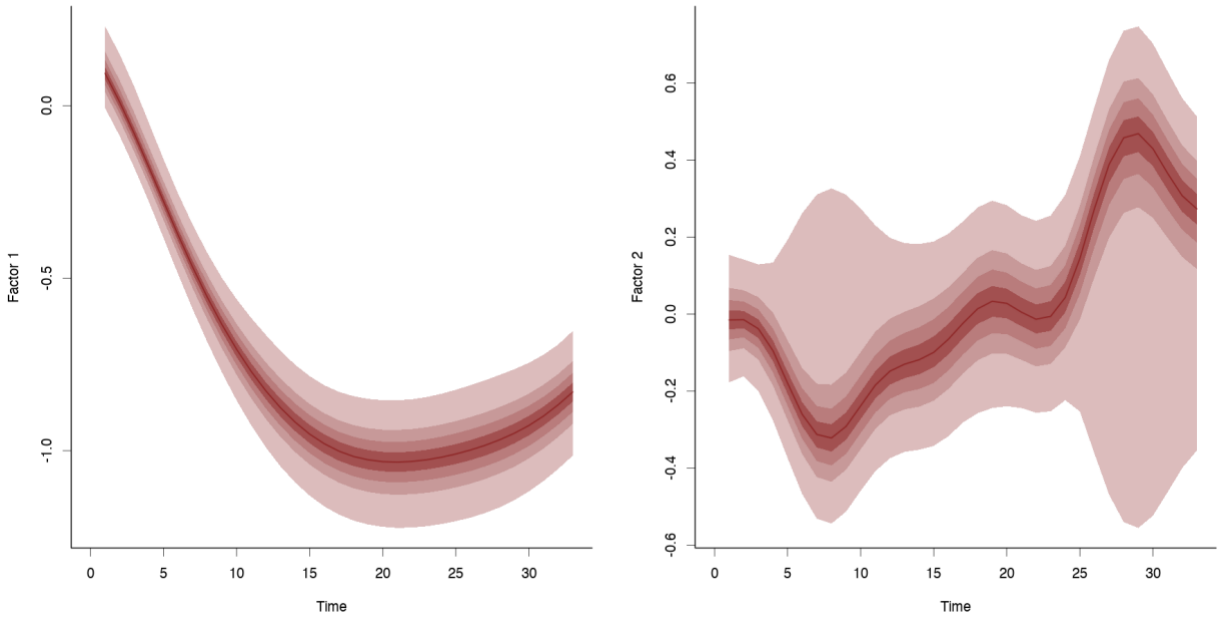

Figure S5. Dynamic latent factors representing a Gaussian process that captured the temporal associations between populations' size fluctuations over time.

The model estimated between 2 and 15 (half the total number of time series) latent variables and increasingly penalized them to squeeze latent variables into flat lines if they did not explain the temporal variation in population sizes, effectively removing them from the model. As a result of this procedure, the model retained 2 latent variables. The shaded ribbons show the posterior quantiles (90%, 60%, 40%, and 20%) and the dark line shows the posterior median.

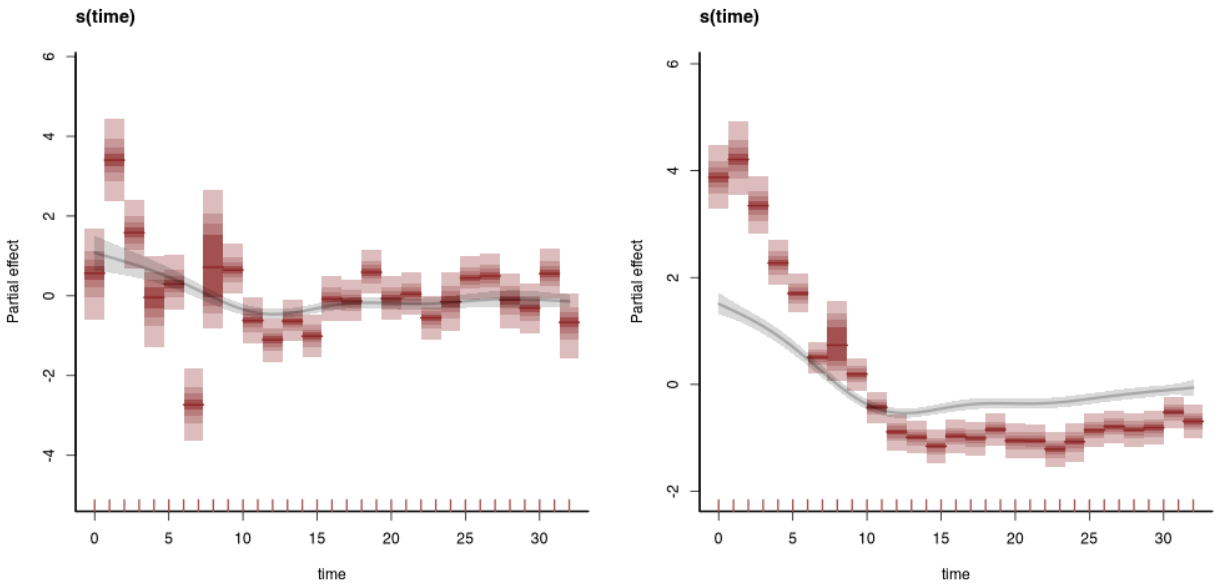

Figure S6. Residual variation explained by the latent trend model.

Residuals of the estimated time smooth (a) with and (b) without the latent trend component of the model.

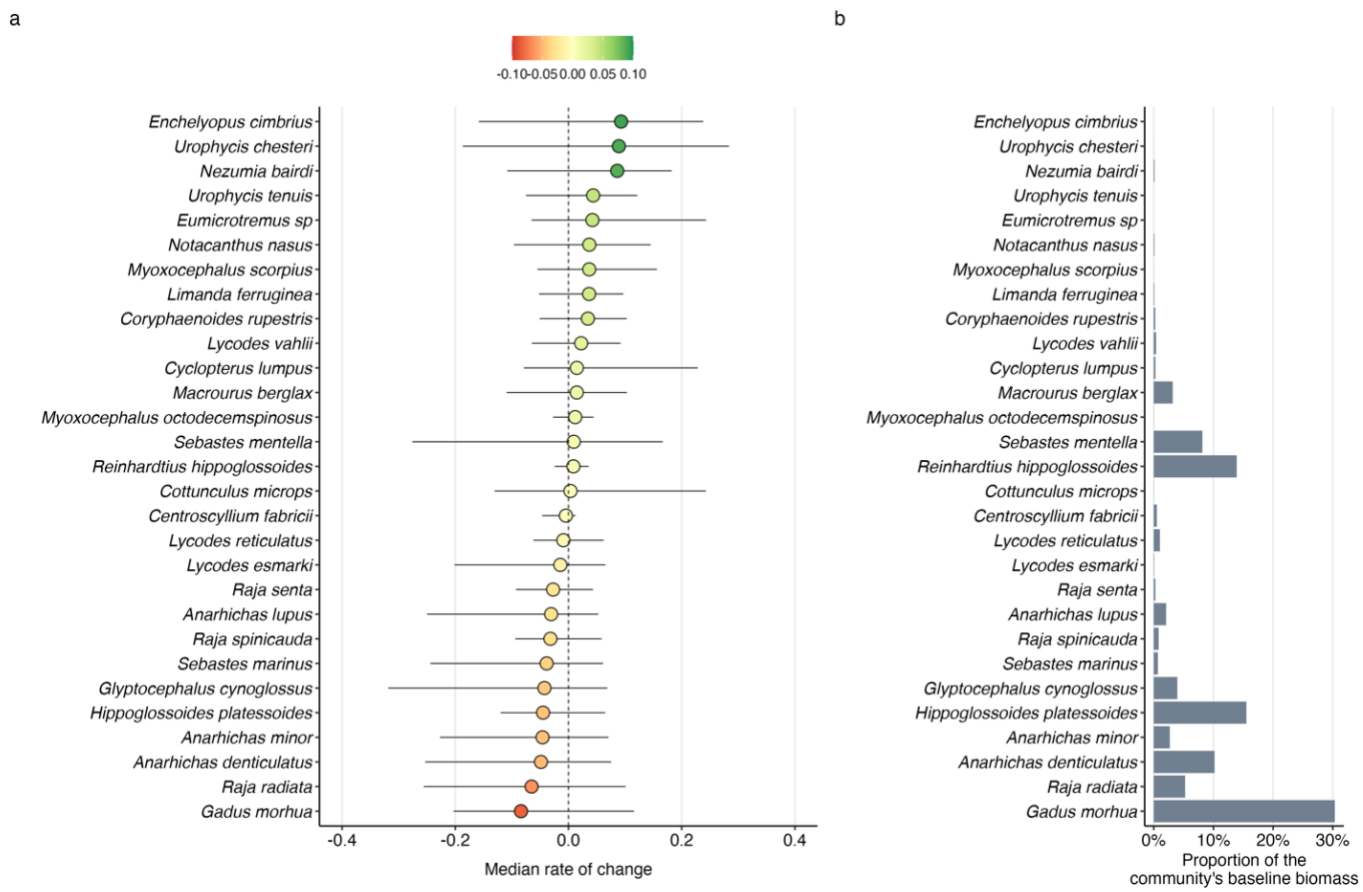

Figure S7. The distribution of the rates of change within species in the Newfoundland shelf groundfish community between 1981 and 2013.

(a) The median estimated rate of annual change for each species in the community between 1981 and 2013, with error bars that show the 90% credible interval around the median. (b) The proportion of the community's baseline biomass that was represented by each species in 1981.

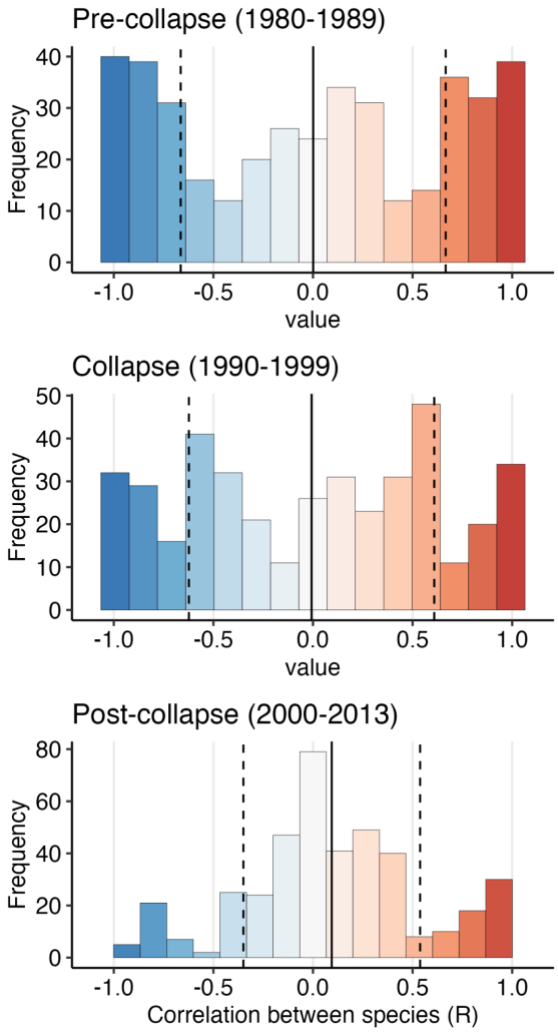

Figure S8. The distribution of short-term species associations in the pre-collapse, collapse, and post-collapse periods for the Newfoundland shelf groundfish community between 1981 and 2013.

Though the average correlation does not change substantially, the distribution of pairwise correlations varies widely between periods. Strong correlations pre-collapse and during the collapse flag unstable community dynamics, where large gains and losses were unfolding rapidly across many species in the community.

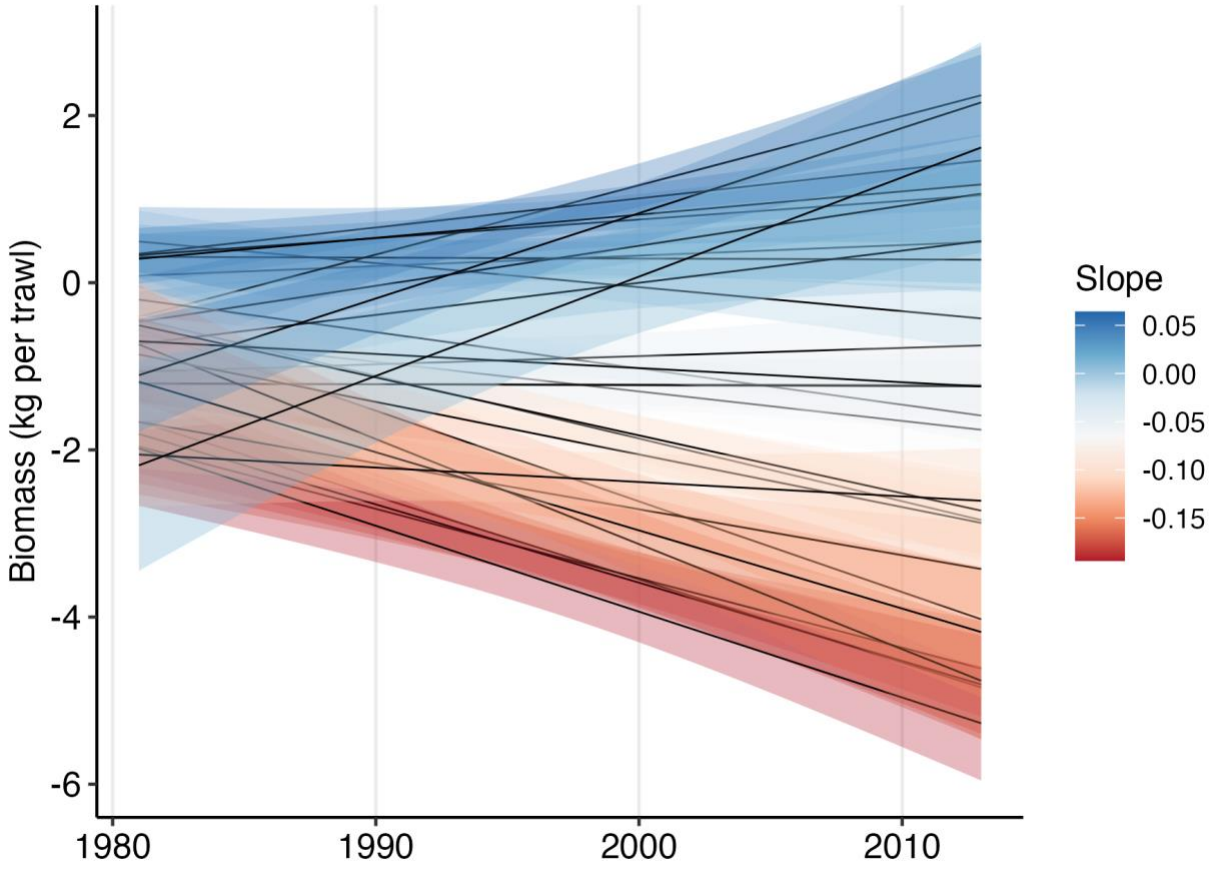

Figure S9. The long-term linear trends of species in the community, which were used to calculate long-term coherence as the pairwise multiplication of species' slopes.

Each line is the estimated trend in a species' biomass, fit as a linear regression whose slope is represented by the colour of the confidence intervals.

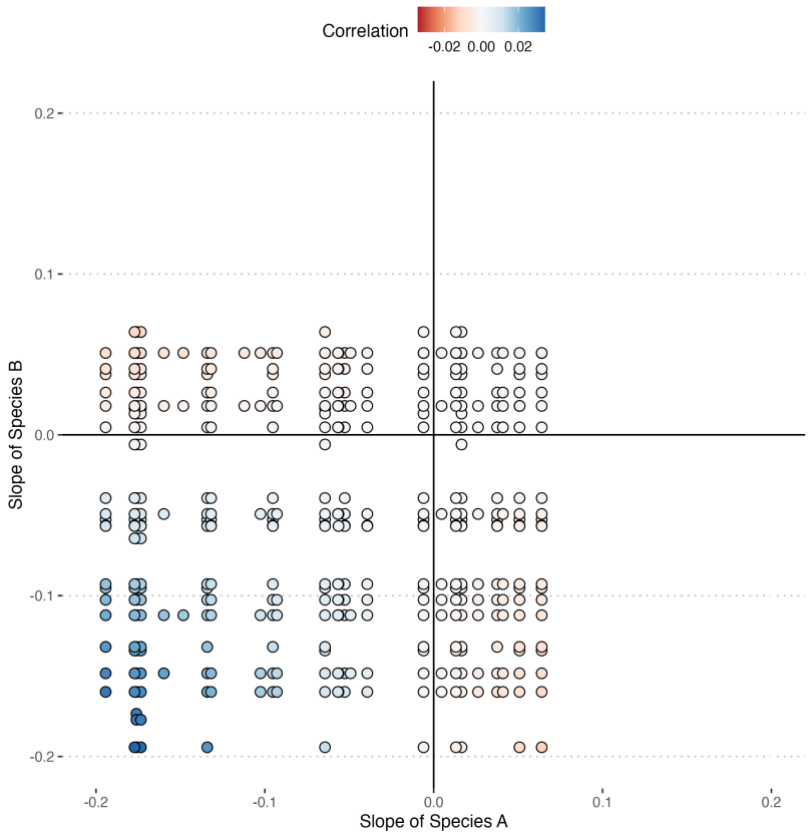

Figure S10. Interpreting long-term species association values to understand long-term changes in community structure and dynamics in the Newfoundland groundfish community between 1981 and 2013.

Long-term species associations were estimated for species pairs as the product of their linear slopes (Fig. S9). The top-left panel and bottom-right quadrant show species pairs where one species' abundance grew while the other declined. The top-right quadrant shows species pairs that both increased in abundance. The bottom-left quadrant signals same-direction declines. Ideally, most species pairs would fall near the (0,0) origin (that is, little long-term change in abundance). Here, the prevalence of species pairs in the bottom-left quadrant signals large, widespread declines that are only partially offset by weaker species growth in the top-left and bottom-right quadrants.